

POLITECNICO DI TORINO

Corso di Laurea Magistrale in Automotive Engineering

Tesi di Laurea Magistrale

# Feasibility analysis of the e-turbo application to a commercial diesel engine vehicle



Relatori:

Prof. Mirko BARATTA

Prof. Daniela Anna MISUL

Prof. Roberto FINESSO

Candidato:

Giuseppe BASSO

Marzo 2018

# Contents

<b>1</b>	<b>Introduction</b>	<b>3</b>
1.1	Vehicle hybridization . . . . .	3
1.2	Turbo compound . . . . .	4
1.3	Simulation software: GT-POWER . . . . .	5
<b>2</b>	<b>Model of the propulsion system</b>	<b>6</b>
2.1	Starting model . . . . .	6
2.2	Model modification . . . . .	7
<b>3</b>	<b>Simulation performed</b>	<b>9</b>
3.1	Turbo matching . . . . .	9
3.2	FGT and EM . . . . .	11
3.3	Accessories division . . . . .	17
3.4	DoE . . . . .	23
<b>4</b>	<b>Conclusion</b>	<b>33</b>
4.1	Final Remarks and future works . . . . .	33
<b>5</b>	<b>Further plots</b>	<b>34</b>
5.1	Turbomatching plots . . . . .	34
5.2	FGT and EM . . . . .	35
5.3	Accessories division . . . . .	35

# List of Figures

1.1	Series hybrid scheme . . . . .	3
1.2	Parallel hybrid scheme . . . . .	4
1.3	turbo compound scheme 1 . . . . .	5
1.4	turbo compound scheme 2 . . . . .	5
2.1	Starting model . . . . .	6
2.2	Accessories submodel . . . . .	7
3.1	Boost pressure . . . . .	10
3.2	Brake mean effective pressure . . . . .	10
3.3	Brake specific fuel consumption . . . . .	11
3.4	Wastegate position . . . . .	11
3.5	Accessories scheme "starting model" . . . . .	11
3.6	Inlet turbine pressure . . . . .	12
3.7	Boost pressure . . . . .	12
3.8	Brake mean effective pressure . . . . .	12
3.9	Net indicative mean effective pressure . . . . .	13
3.10	Brake specific fuel consumption . . . . .	13
3.11	System efficiency . . . . .	13
3.12	Electric power at the battery . . . . .	14
3.13	Accessories scheme 2 . . . . .	14
3.14	Inlet turbine pressure . . . . .	15
3.15	Boost pressure . . . . .	15
3.16	brake mean effective pressure . . . . .	15
3.17	Net indicated mean effective pressure . . . . .	16
3.18	Brake specific fuel consumption . . . . .	16
3.19	System efficiency . . . . .	16
3.20	Electric power at the battery . . . . .	17
3.21	WHTC working points . . . . .	18
3.22	Accessories power . . . . .	19
3.23	Inlet turbine pressure . . . . .	19
3.24	Boost pressure . . . . .	20
3.25	Brake mean effective pressure . . . . .	20
3.26	Net indicated mean effective pressure . . . . .	21
3.27	Brake specific fuel consumption . . . . .	21
3.28	System efficiency . . . . .	22
3.29	Electric power . . . . .	22
3.30	Brake mean effective pressure . . . . .	24
3.31	Brake specific fuel consumption . . . . .	24
3.32	System efficiency . . . . .	25
3.33	Electric power to the battery . . . . .	25

3.34	Brake specific fuel consumption 1800 x 4.5 . . . . .	26
3.35	Brake specific fuel consumption 1800 x 9 . . . . .	27
3.36	Brake specific fuel consumption 3250 x 4 . . . . .	27
3.37	Brake specific fuel consumption 3250 x 8 . . . . .	28
3.38	System efficiency 1800 x 4.5 . . . . .	28
3.39	System efficiency 1800 x 9 . . . . .	29
3.40	System efficiency 3250 x 4 . . . . .	29
3.41	System efficiency 3250 x 8 . . . . .	30
3.42	Electric power 1800 x 4.5 . . . . .	30
3.43	Electric power 1800 x 9 . . . . .	31
3.44	Electric power 3250 x 4 . . . . .	31
3.45	Electric power 3250 x 8 . . . . .	32
5.1	Indicative mean effective pressure . . . . .	34
5.2	Lambda coefficient . . . . .	34
5.3	Maximum pressure in combustion chamber . . . . .	35
5.4	Inlet turbine temperature . . . . .	35
5.5	Total power dissipated . . . . .	35
5.6	Maximum pressure in combustion chamber . . . . .	36
5.7	Inlet turbine temperature . . . . .	36
5.8	Total power dissipated . . . . .	36
5.9	Maximum pressure in combustion chamber . . . . .	37
5.10	Inlet turbine temperature . . . . .	37
5.11	Total power losses . . . . .	38
5.12	Pumping mean effective pressure . . . . .	38
5.13	Lambda coefficient . . . . .	39



# List of Tables

2.1	PID factors . . . . .	7
2.2	different mass multiplier . . . . .	8
2.3	Alternator data . . . . .	8
3.1	Working points . . . . .	9
3.2	Rack position "base model" . . . . .	10
3.3	Working points added . . . . .	18
3.4	Rack Position . . . . .	19
3.5	DoE working points FGT . . . . .	23
3.6	DoE working points VGT . . . . .	23

# Bibliography

- [1] *Thermoelectrics for Automotive Waste Heat Recovery Department of Energy*, FANKAI MENG, LINGEN, CHEN YUANLI, FENG BING XIONG, (2017)
- [2] *A review and future application of Rankine Cycle to passenger vehicles for waste heat recovery* FENG ZHOU SHAILESH N.JOSHI RAPHAEL RHOTE VANEY ERCAN M. DEDE (2017)
- [3] *Feasibility study of an electrified propulsion system using an electric turbo compound* LEANDRO CORRADO TERZO (2017)

# List of abbreviations

bmep Brake mean effective pressure  
BSFC Brake specific fuel consumption  
EM Electric motor  
FGT Fixed geometry turbine  
fmep Friction mean effective pressure  
ICE Internal combustion engine  
imep Indicative mean effective pressure  
pmep Pumping mean effective pressure  
VGT Variable geometry turbine

# Acknowledgements

Questa tesi è dedicata soprattutto alla mia famiglia: mamma, papà, Carmela, Antonietta, Luigi, mio cognato Pasquale e il mio nipotino Antonio. Grazie per avermi supportato in questi anni e incoraggiato a far sempre quel che ho desiderato non impedendomi nulla. Grazie ai miei coinquilini: Agostino, Mauro, German, Daniele e i due Stefano. Con loro ho sempre sentito casa una vera "Casa", non dimenticherò mai tutte le nostre avventure. Grazie al gruppo Geriatria: Putina, Davide, Alessandra, Alida, Chiara, Ciccio, Emilia, Flavia, Gianluca, Gianni, Marco, Giuglia, Giusy, Leandro, Silvia, Stefania, Valentina. Siete stati i primi che ho conosciuto in questa nuova esperienza e avete reso questo percorso speciale. Grazie ai miei amici di sempre: Biagio, Antonio, Alessio e Francesca. Grazie per avermi tirato su nei momenti di sconforto ed essere cresciuti insieme. Grazie ad Angela e Livia che mi hanno accolto sempre in casa loro tutti i giorni per due anni (prima o poi vi pagherò una parte dell'affitto) insieme a Mattia e Eleonora. Grazie al Team H2politO, grazie alla prof Carello, ai responsabili che mi hanno accolto nel primo anno, Grazie ai training che mi hanno seguito nel secondo anno e soprattutto grazie ai ragazzi che sono stati responsabili con me: Mike, Alice, Giulio, Mariano, Fabio, Marco, Davide, Pietrino, Matilde, Danilo. Con voi ho passato un intero anno dove ne abbiamo viste di tutti i colori, con momenti che passavano dal tragicomico alla disperazione più assoluta. È stato l'anno più movimentato da quando vivo a Torino. Grazie a tutti quelli che ho incontrato in questi anni e che mi hanno dato qualcosa.

# Abstract

The aim of this master thesis work is to study the feasibility to power supply accessories (fuel pump, oil pump and water pump) thanks to the energy recovered by an e-turbo (electrified turbocharging) system and its potential to increase the efficiency of the powertrain unit.

The engine used for the study is a 4-cylinder diesel engine mounted on a commercial vehicle.

The assessment was performed using GT-Power software with a model of the engine validated by the manufacturer. The electrified accessories model has been developed in a previous thesis. The first step of this work has been to substitute the variable geometry turbine (VGT) of the real engine with a fixed geometry turbine (FGT). For the analysis fifteen working points have been taken into account, at five different speed and three different load conditions.

The results indicate that only at full load and high speed conditions the energy recovered from the exhaust gases is enough to drive all the accessories, however without any increase in the powertrain efficiency. The oil and water pump can be electrified using a VGT configuration while using a FGT configuration a calibration of boost pressure is needed. In both cases the efficiency of the powertrain does not increase in a significant way. Moreover a DoE analysis has been done in order to explore the possibility of increasing the powertrain efficiency by changing the main engine calibration parameters, when the e-turbo system is adopted. However, it was found that the achievable improvement is very small.

In general, it was found that the small efficiency improvements which can be achieved using the e-turbo system are due to the excessive exhaust manifold back pressure which affects negatively the engine efficiency, due to an increase in the pumping losses.

# Chapter 1

## Introduction

### 1.1 Vehicle hybridization

Stringent environmental regulations are pushing toward even more electrified powertrain. In next years ICE will be assisted by an electric motor of different size even more. Hybrid electric vehicles can be divided in two main categories:

- series hybrid,
- parallel hybrid.

The former category uses the EM only to push the vehicle on the road, while the ICE has the task to produce electrical energy required by the EM. This type of powertrain can give some advantages in terms of efficiency for the ICE, since that the engine can work at one specific point and all the pieces and parameters are optimized. A scheme of series hybrid powertrain is represented in the figure 1.1:

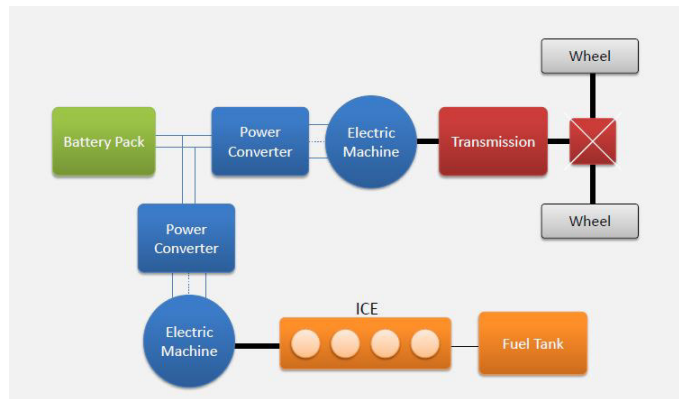


Figure 1.1: Series hybrid scheme

In latter category both EM and ICE provide the needed power to move the vehicle. In this case the EM usually assist the ICE in transient phases and it recovers kinetic energy during braking. Parallel hybrid powertrain scheme is shown in figure 1.2:

In last years automotive OEMs are switching to hybrid vehicles in a progressive way. As a matter of fact several of them are introducing some devices that lead the powertrain toward hybridization as the BSG (belt starter generator) and the turbo electrically assisted (that is the object of this work).

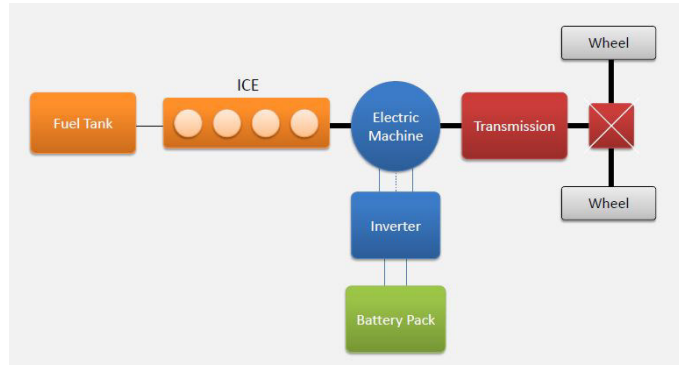


Figure 1.2: Parallel hybrid scheme

## 1.2 Turbo compound

In common internal combustion engine, about one third of the chemical energy of fuel is wasted in exhaust gases. There are three main technologies to recover in part this energy:

- Thermoelectric generator (TEG),
- Rankine cycle,
- Turbo compounding.

TEG converts directly the heat flux in electric energy through the Seebeck effect. The greatest challenge to the scaling of TEG from prototyping to production has been the cost of the underlying thermoelectric materials. Since the early-2000s, many research agencies and institutions poured large sums of money into advancing the efficiency of thermoelectric materials. While efficiency improvements were made in materials such as the half heuslers and skutterudites, like their predecessors bismuth telluride and lead telluride, the cost of these materials has proven prohibitive for large-scale manufacturing [1].

Rankine cycle uses thermodynamic processes to recover energy from the exhaust gases. Rankine Cycle (RC) is a thermodynamic cycle that converts thermal energy into mechanical work, which is commonly found in thermal power generation plants. Recently, there have been many studies focusing on applying Rankine Cycle to recover low-grade waste heat. On-road vehicles, which convert around one third of the fuel energy into useful mechanical energy for propulsion, are moving energy conversion systems that generate considerable waste heat. It is found from prior research that the Rankine Cycle has great potential in automobile waste heat harvesting applications. However, in contrast with other low-grade waste heat applications, vehicles have limited space for the RC system integration, and the waste heat is relatively unsteady [2]. In turbo compound a turbine is used to transform the energy of exhaust gases in mechanical power. The turbine can be linked to the crankshaft (mechanical turbo compound) through a series of gears, or can be coupled to an electric motor/generator (electric turbo compound). The last configuration can be implemented in two ways, and they are represented in the figures 1.4:

In first configuration the EM works as a generator only since that it is no coupled to the compressor and so the motor mode is no useful. In the second one EM is integrated in the turbocompressor and motor mode is active in order to reduce the turbo lag during transient phase. In this thesis will be simulated the last configuration and it will be studied the possibilities to take advantage of the electric energy recovered during the generator mode so that the efficiency of whole system will increase.

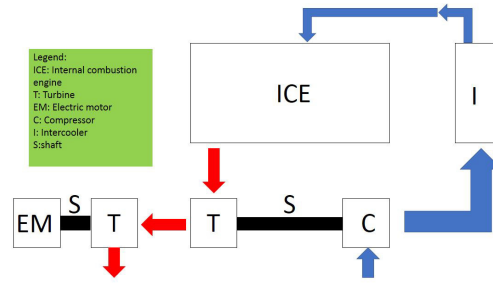


Figure 1.3: turbo compound scheme 1

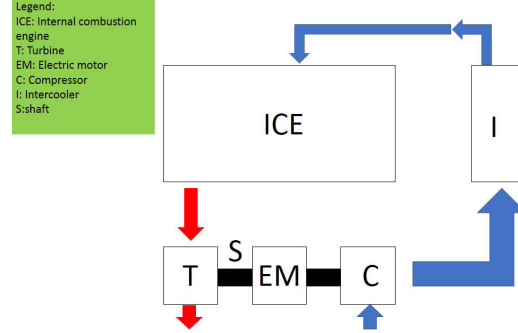


Figure 1.4: turbo compound scheme 2

### 1.3 Simulation software: GT-POWER

- This feasibility study has been conducted using the simulation software GT-Power2(v7.5.0, Gamma Technologies, LLC., Westmont, IL, USA). GT-Power is the industry-leading software for engine simulation with a detailed cylinder model and combustion analysis; it is recognised worldwide as the Industry Standard for system simulations and is used by all major engine manufacturers and vehicle OEMs. It allows to build versatile multi-physics models via embedded libraries (flow, acoustics, thermal, mechanical, electric and electromagnetic, chemistry and controls) and then to perform accurate mono-dimensional fluid-dynamics simulations. [3]



## Model of the propulsion system

## 2.1 Starting model

The modelled engine belongs to a commercial light duty vehicle: it is a 3.0 litres diesel engine with 16 valves and 4 cylinders, equipped with a variable geometry turbine (VGT) and common rail high pressure injection. It provides 400 Nm of torque in the speed range  $1250 \div 3000$  rpm and a nominal power equal to 130 kW between  $3200 \div 3500$  rpm. [3]

The engine model has been built during a previous thesis work [December, 2017] and has been adopted as a starting point of this work; the model is represented in the figure 2.1:

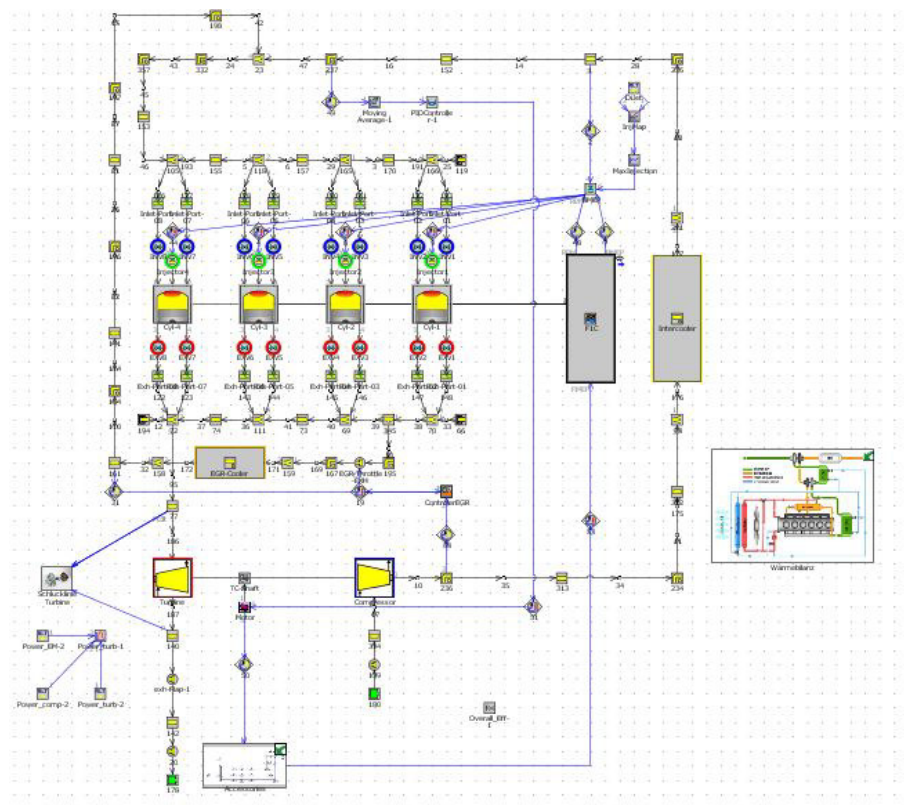


Figure 2.1: Starting model

In this model the VGT turbine has a fixed rack position (0.321) in order to simulate a fixed geometry turbine. The disadvantages about turbo lag in a traditional turbocompressor equipped with a FGT are compensated by the electric motor mounted on its shaft. Indeed the EM is controlled with a PID controller that manages the power delivered/absorbed in order to reach

the boost target. The values of three PID controller factors are shown in table 2.1:

Proportional	Integral	Derivative
38110.594	141378.01	0

Table 2.1: PID factors

The EM simulated in this work has a nominal torque of 1 Nm. However the rack position chosen, combined to the braking torque of the EM in generator mode, causes an excessive back pressure to the ICE. This phenomenon decrease dramatically the system efficiency. Data of the previous thesis work confirm that this configuration is no optimal: the starting model has obtained a fuel consumption of 5.9% higher than the base model (in base model the turbocompressor is a traditional one with the VGT that works thanks a PID controller to reach the boost target). About the fmep (friction mean effective pressure) a 'subassembly' has built so to split the several accessories. The image 2.2 shows it:

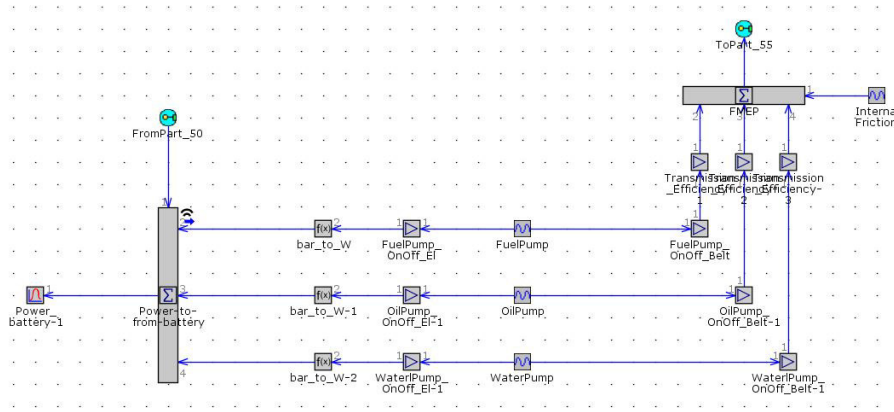


Figure 2.2: Accessories submodel

With this subassembly it is possible to simulate both accessories powered by electricity or through the internal combustion engine and to understand the influence of each accessory on fmep and engine efficiency.

## 2.2 Model modification

As first step the VGT turbine has been replaced with a FGT one. The FGT is a turbine equipped on a 2.0 litres engine and the turbo matching has been performed changing the parameter 'mass multiplier'. It permits to simulate turbines with different size and same performance of original one. The values of 'mass multiplier' tested are shown in table 2.2:

About the fmep, the alternator has been added to the accessories. The alternator simulated is 'Alternator 150A PSA DV4'. Actually this is no the alternator mounted on our engine, but it is of a similar engine and vehicle, so the adsorbed power is very close to the real one. The choice to add the alternator has been taken because one wanted to study the possibility to substitute the alternator with electric turbo to satisfy the electrical loads power required. The pulley ratio between engine and alternator is 2.75, so the alternator data are represented in the table 2.3:

	mass multiplier
1	0.8
2	0.9
3	1
4	1.1

Table 2.2: different mass multiplier

Engine speed [rpm]	Power [kW]	fmep [bar]
1000	1.02	0.41
1200	1.14	0.38
1400	1.25	0.36
1600	1.36	0.34
1800	1.46	0.33
2000	1.57	0.31
2250	1.69	0.3
2500	1.81	0.29
2750	1.92	0.28
3000	2.03	0.27
3250	2.13	0.26
3500	2.23	0.25

Table 2.3: Alternator data

## Chapter 3

# Simulation performed

### 3.1 Turbo matching

As said before, the first step of this work has been to substitute the VGT of real engine with a FGT. For this choice three different turbine have been taken into account:

- FGT of a 2.0 litres engine with mass multiplier 0.8,
- VGT of starting model with the fixed rack position of 0.321 (from previous work),
- FGT of a 8.0 litres engine with mass multiplier 0.4.

All the simulation have been performed without the EM and with a control on the wastegate valve to reach the boost target in the several working points tested.

The working points used in this step of the study were at 50% and 100% of load, with the speed range from 1200 rpm to 3250 rpm. The respective bmep (brake mean effective pressure) of the points is shown in the table 3.1:

In the charts 3.1-3.4 are represented the main parameters in the several configurations.

From the three parameters shown it is possible to understand what is the best turbine. "base model" is the engine configuration without electric motor mounted on the turbo and VGT working properly to reach the target boost. Comparison has been done with this configuration because it is better than "starting model" one in which there are the EM and VGT in fixed position.

Engine speed [rpm]	bmep 50% [bar]	bmep 100% [bar]
1200	7.3	14.7
1800	9	18.1
2250	9	18
2750	9	17.9
3250	8	15.4

Table 3.1: Working points

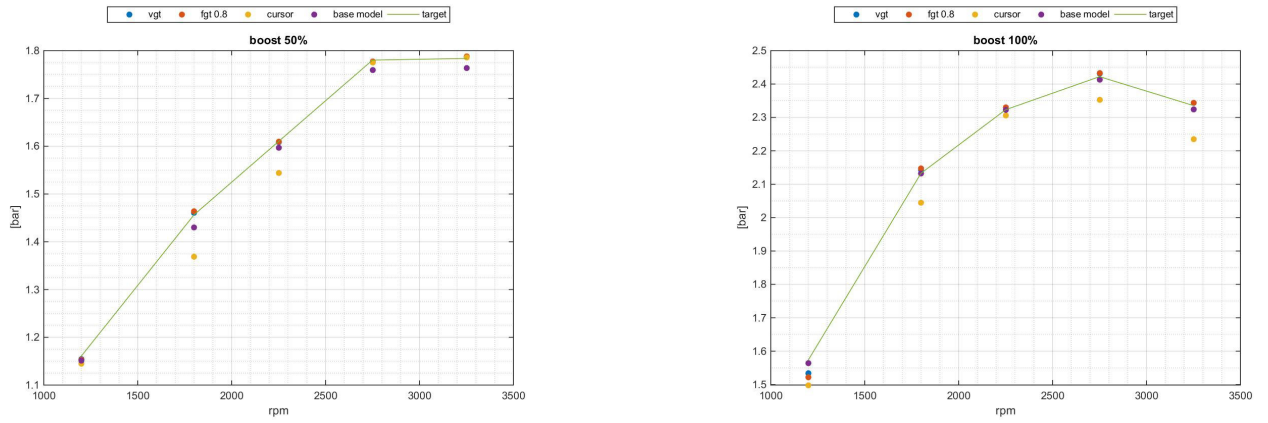


Figure 3.1: Boost pressure

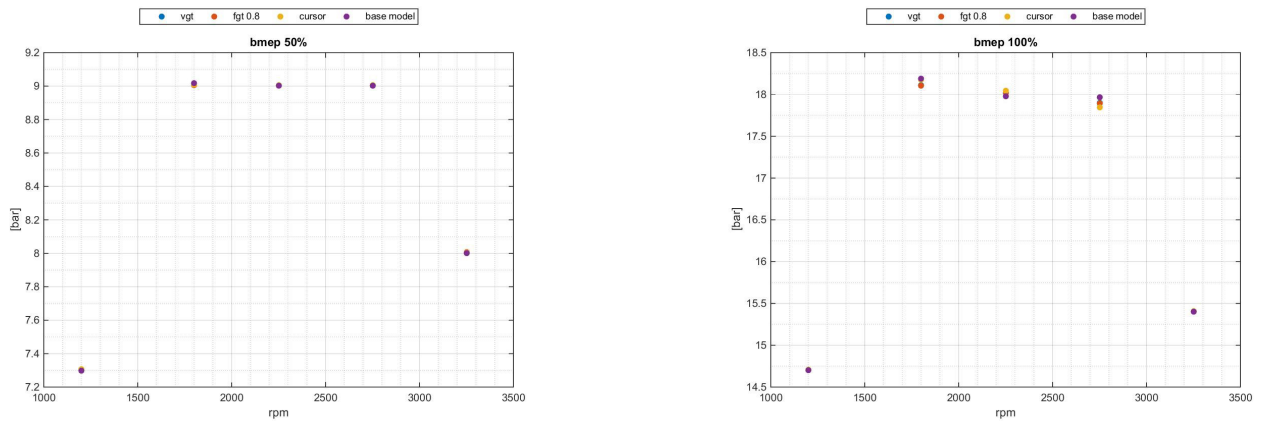


Figure 3.2: Brake mean effective pressure

Observing boost data it is possible to exclude "cursor" (FGT of 8.0 litres engine). Indeed with this turbine the boost target is not reached in the half of cases. This no matching in 3/5 cases happens with the wastegate valve closed. This means that the turbine is not able to extrapolate sufficient power from exhaust gases to satisfy boost target.

Considering the other two turbines (that respect both bmep and boost targets) one analyse the graphs where BSFC (brake specific fuel consumption) are plotted. About the VGT, an higher BSFC than "base model" occurs, because our fixed position (0.321) is smaller than all rack position of "base model" (Table 3.2). Indeed the smaller this parameter is, the more back pressure increases, with penalties in engine efficiency. This phenomenon is more detrimental with high engine speeds and high loads.

Taking into account the FGT, it is possible to note that from 1200 rpm to 2250 rpm and at

	50%	100%
1200	0.37	0.32
1800	0.35	0.40
2250	0.40	0.48
2750	0.46	0.61
3250	0.56	0.64

Table 3.2: Rack position "base model"

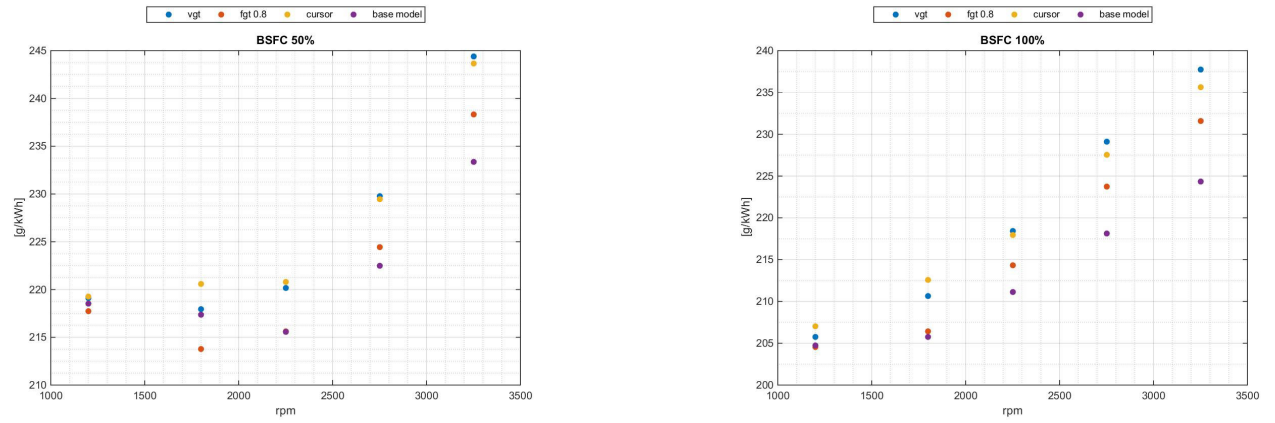


Figure 3.3: Brake specific fuel consumption

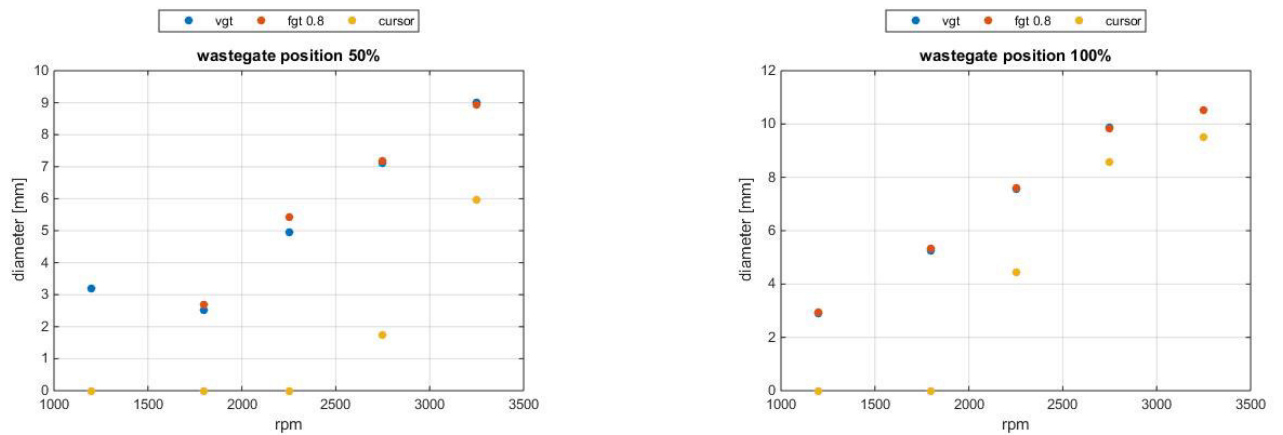


Figure 3.4: Wastegate position

half load there is a lower BSFC than "base model", after that the efficiency of this configuration is worse. In full load conditions the difference between two models is higher than in half load conditions.

Analysing these data is clear that the better configuration with a fixed geometry turbine is the FGT of 2.0 litres engine.

## 3.2 FGT and EM

In the second step of this work the e-turbo configuration with the FGT turbine has been simulated. The accessories are electrically driven as in "starting model" (figure 3.5):

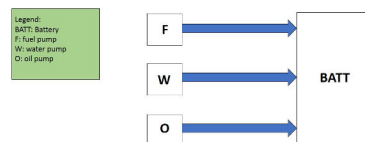


Figure 3.5: Accessories scheme "starting model"

Should be noted that in this configuration the alternator is no considered yet. They have been simulated four different configurations shown in table 2.2 and with the same electric motor and PID controller. In next figures the main data will be represented (from figures 3.6 to 3.12).

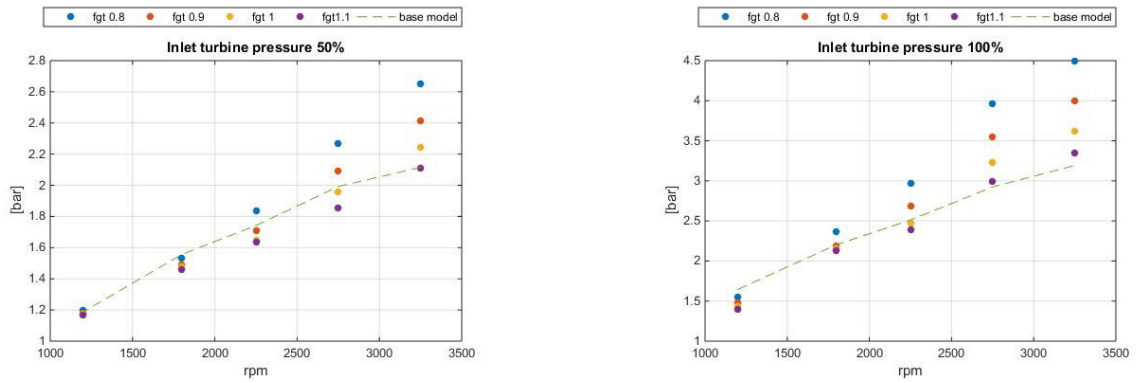


Figure 3.6: Inlet turbine pressure

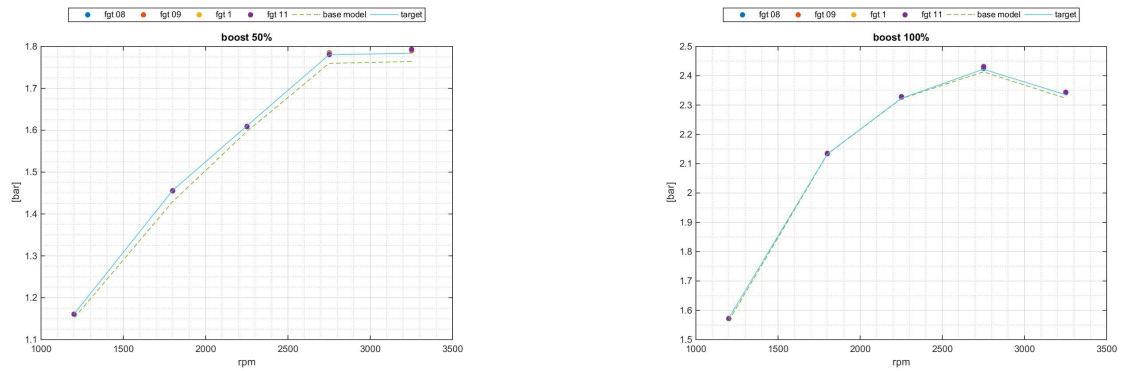


Figure 3.7: Boost pressure

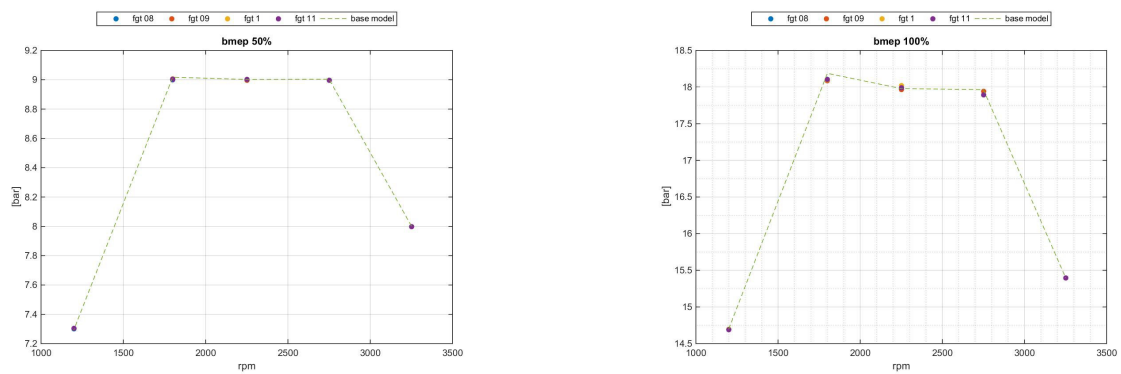


Figure 3.8: Brake mean effective pressure

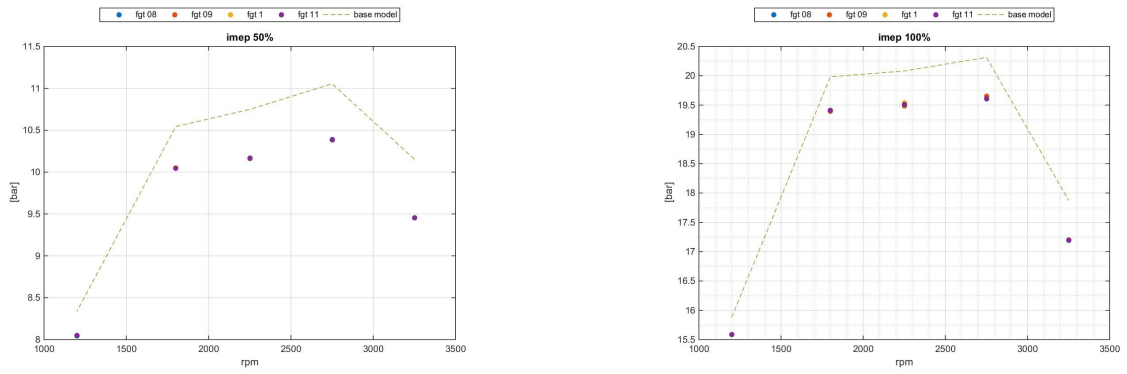


Figure 3.9: Net indicative mean effective pressure

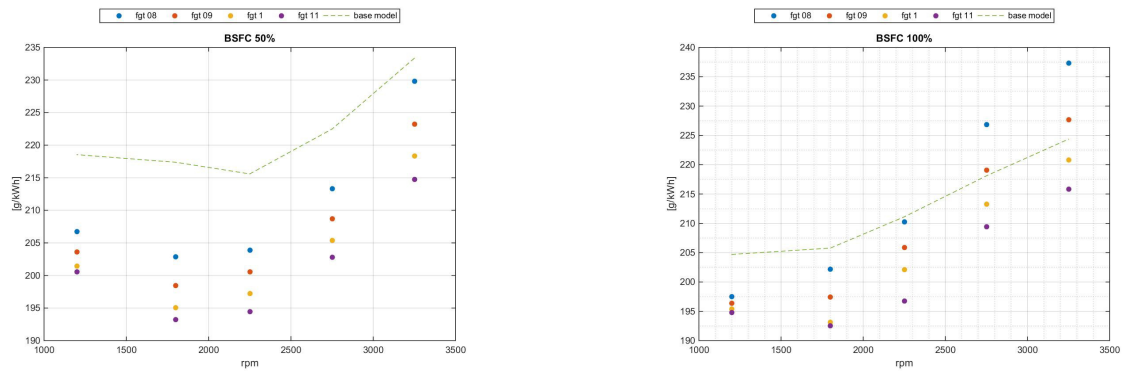


Figure 3.10: Brake specific fuel consumption

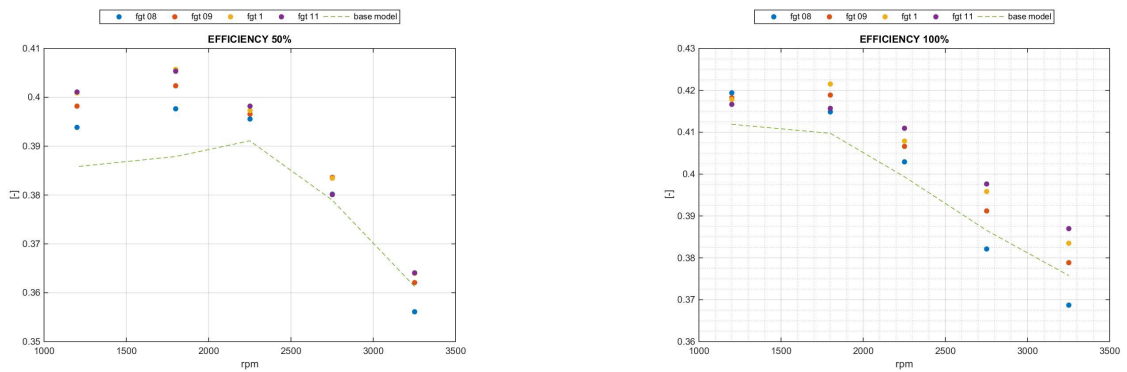


Figure 3.11: System efficiency



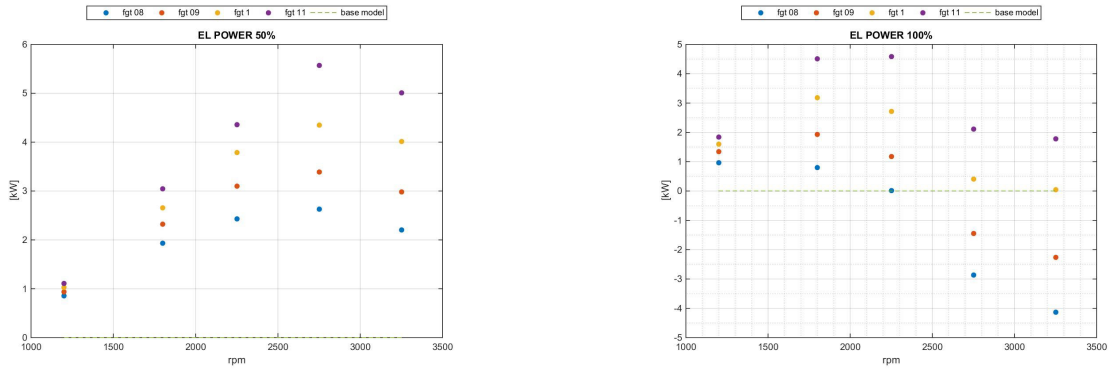


Figure 3.12: Electric power at the battery

From charts 3.6 it is possible to deduct that the configuration with mass multiplier 0.8 generates a back pressure higher than "base model" from 2250 rpm at half load and from 1800 rpm in full load. The configuration that reaches similar back pressure to "base model" is the FGT 1.1 configuration. The bmep and boost target are respected in all configurations. The imep are all equal (fmep are the same for the four configurations) and are lower than "base model" because the accessories are powered electrically in e-turbos configurations. About the BSFC, at 50% of load all the configuration have lower values than reference model, while at full load and high engine speeds (from 2750 rpm) the FGT 0.8 and FGT 0.9 have a fuel consumption higher than the "base model". The efficiency of whole system is represented in figures 3.11 where only the FGT 0.8 configuration has in some points an efficiency lower than "base model". This condition occurs in three points: 3250 rpm 50%, 2750 rpm and 3250 rpm 100%.

In graphics 3.12 the power required/stored to the battery is represented (the power is required when it is positive, it is negative when it is stored). At half load all the configurations require power to the battery, while at full load the FGT 0.8 and FGT 0.9 configurations are able to store energy from 2750 rpm. This means that also if the engine has a better efficiency in almost all points with the e-turbos configurations, must be observed that the system is no self-sustaining because the energy is required in most of occasions.

After the analysis of these simulations, has been decided to perform an other test with the accessories linked in accordance to the figure 3.13:

The aim of this test is to understand if there are some advantages in terms of efficiency using

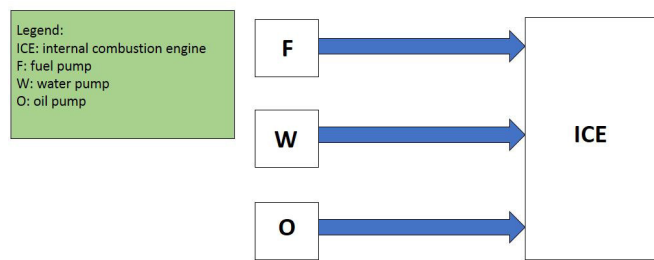


Figure 3.13: Accessories scheme 2

e-turbo on traditional configuration engine (accessories linked to the crankshaft through a belt pulley mechanism) and the quantity of electric energy that can be recovered from exhaust gases. In next graphs the main parameters will be represented (from figures 3.14 to 3.20):

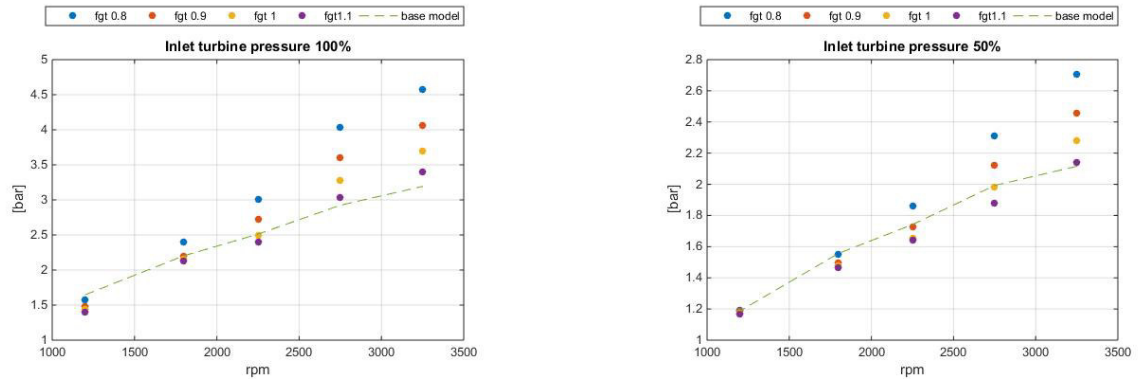


Figure 3.14: Inlet turbine pressure

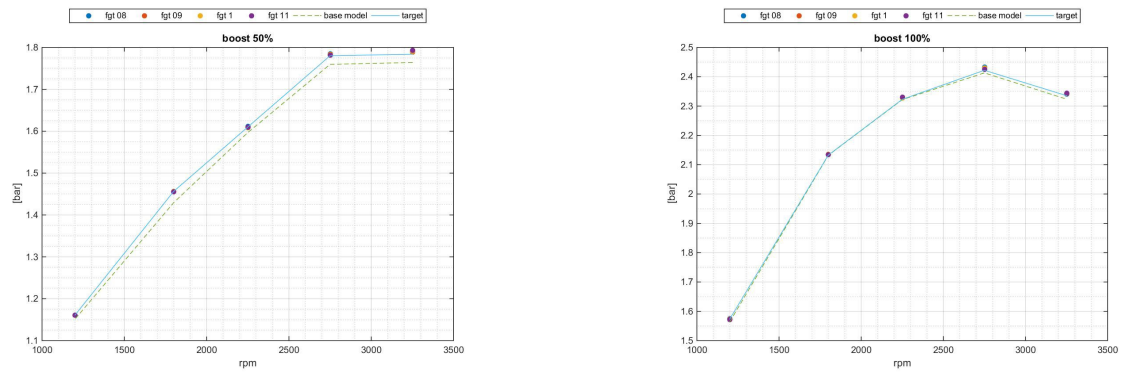


Figure 3.15: Boost pressure

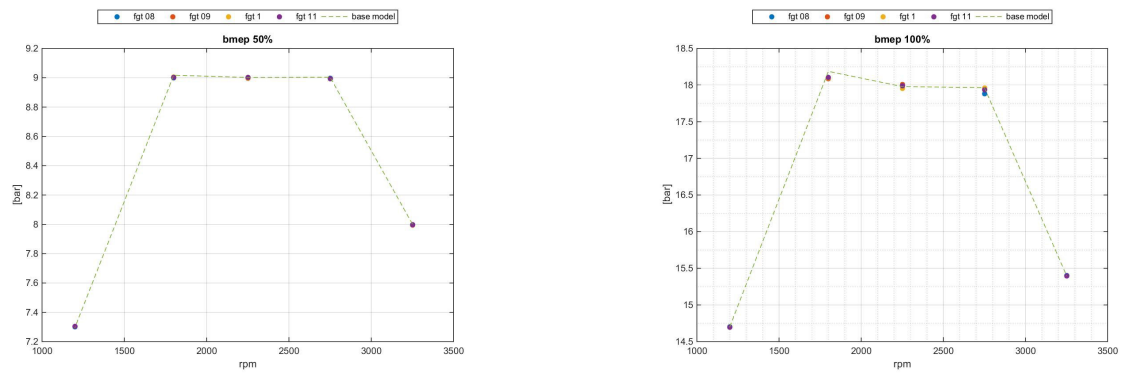


Figure 3.16: brake mean effective pressure

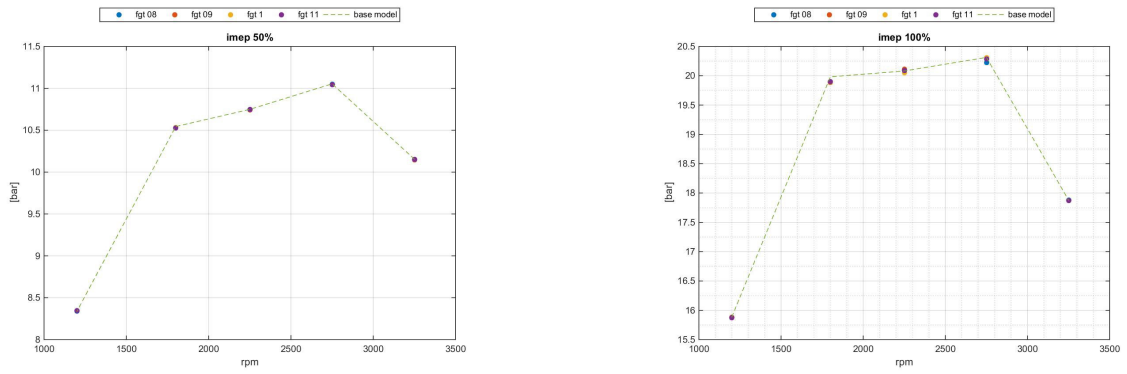


Figure 3.17: Net indicated mean effective pressure

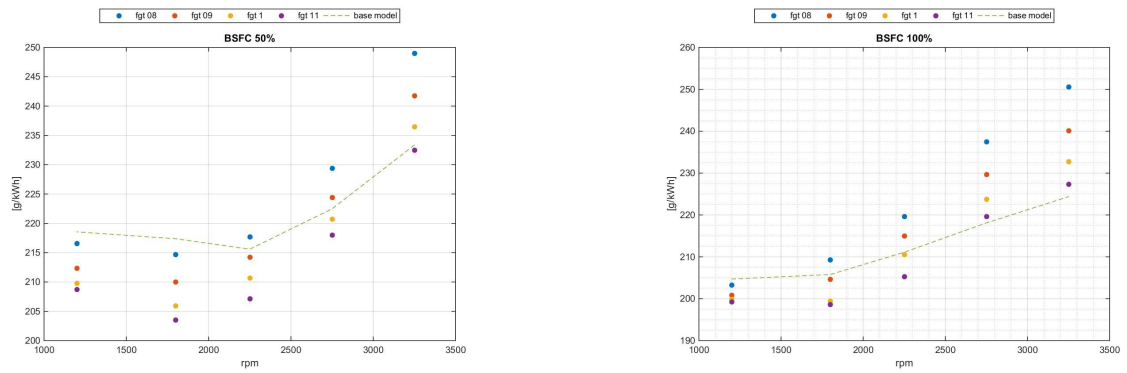


Figure 3.18: Brake specific fuel consumption

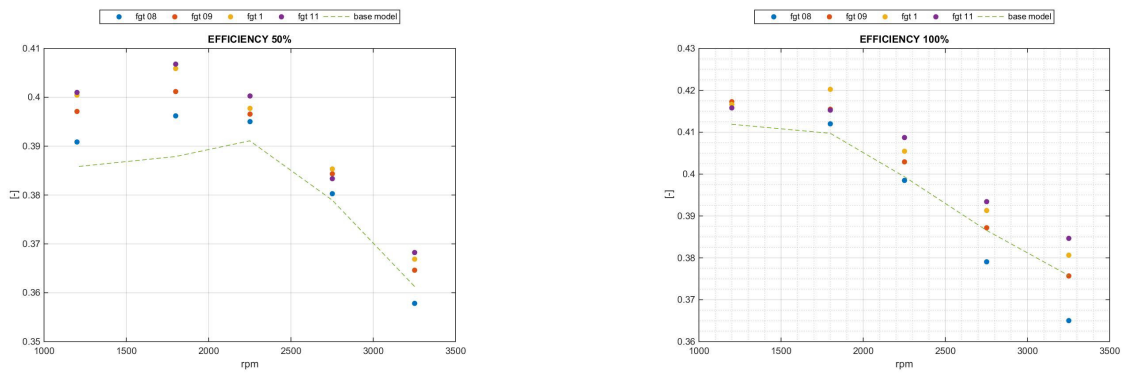


Figure 3.19: System efficiency

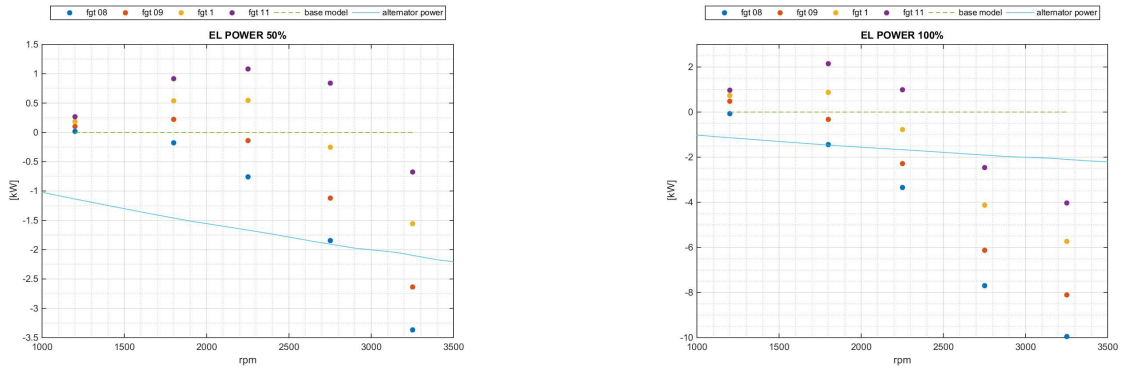


Figure 3.20: Electric power at the battery

About inlet turbine pressure no changes are noted, because of the same working points of the turbines. imep are all equal to the "base model" due to the fact that in these simulations the fimep are the same for all configurations. Concerning the BSFC, at 50% load and low-medium rpm, there is a lower fuel consumption than "base model". This effect is more evident for greater turbines (indeed they generate a lower back pressure). At high engine speeds the fuel consumptions become higher for FGT 0.8 FGT 0.9 and FGT 1 (last one only at 3250 rpm). At full load the trend is the same, with smaller differences at low speeds and greater ones at high engine speeds. Efficiencies of all configurations are higher than "base model" at half load, exception for the FGT 0.8 at 3250 rpm where the efficiency is slightly lower. At 100% of load the advantage is minor and the FGT 0.8 has 2 points in which the efficiency is lower than "base model". The electric power recovered increases with smaller turbines (graphs 3.20). On the same plot, power required by the alternator is represented. At half load only FGT 0.8 and FGT 0.9 at 3250 rpm produce enough power to substitute the alternator, while at full load and high speeds this condition is reached with all the configurations.

However considering the low percentage of last condition during real usage and in homologation cycle, it is clear that there are no possibilities to substitute the alternator with e-turbo.

### 3.3 Accessories division

From last results some changes in model were performed:

- five working points have been added, corresponding at same speeds and 25% of load,
- alternator has been inserted to understand the influence on fuel consumption,
- next simulations were performed with FGT 0.9 and VGT.

The five working points are listed in Table 3.3:

These working points have been added in order to have a wider vision of the engine and to understand better if the configuration taken into account could give some advantages on the WHTC (World Harmonized Transient Cycle) without perform a simulation, that it needs a lot of time. A chart representing working points of WHTC is figure 3.21.

Considering previous simulation performed, it has been decided to use for next tests the FGT 0.9, because it reaches a good trade off between energy recovered and gain in efficiency. About

Engine speed [rpm]	bmep [bar]
1200	3.6
1800	4.5
2250	4.5
2750	4.5
3250	4

Table 3.3: Working points added

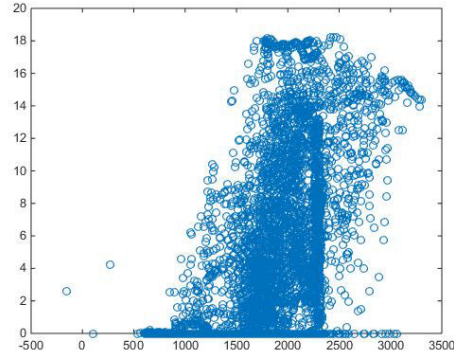
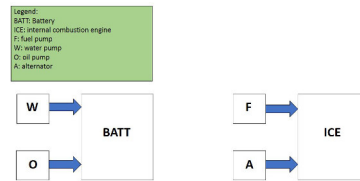


Figure 3.21: WHTC working points

the VGT, analysing the data of last tests it emerged that at low loads and speeds the smaller turbines have lower differences in fuel consumption respect to the greater ones, but recover energy. So the idea is to assign different rack position for different engine speeds and loads to obtain sufficient electric energy and good efficiency.

there is no PID controller for the rack position, but a map (Table 3.4) that is built performing several simulations in order to have the higher efficiency and the necessary electrical energy.

Considering the power absorbed from every accessory (Figures 3.22 ) and the electrical power available from the e-turbo in last simulation (figure 3.20), it was decided to link the accessories as follows:



Simulations have been performed and the results are in graphs from figure 3.23 to 3.29:

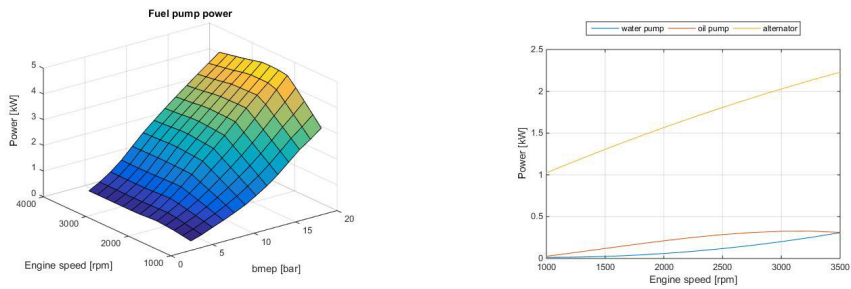


Figure 3.22: Accessories power

rpm	load 25%	load 50%	load 100%
1200	0.22	0.32	0.42
1800	0.22	0.32	0.42
2250	0.22	0.32	0.45
2750	0.25	0.35	0.50
3250	0.30	0.37	0.60

Table 3.4: Rack Position

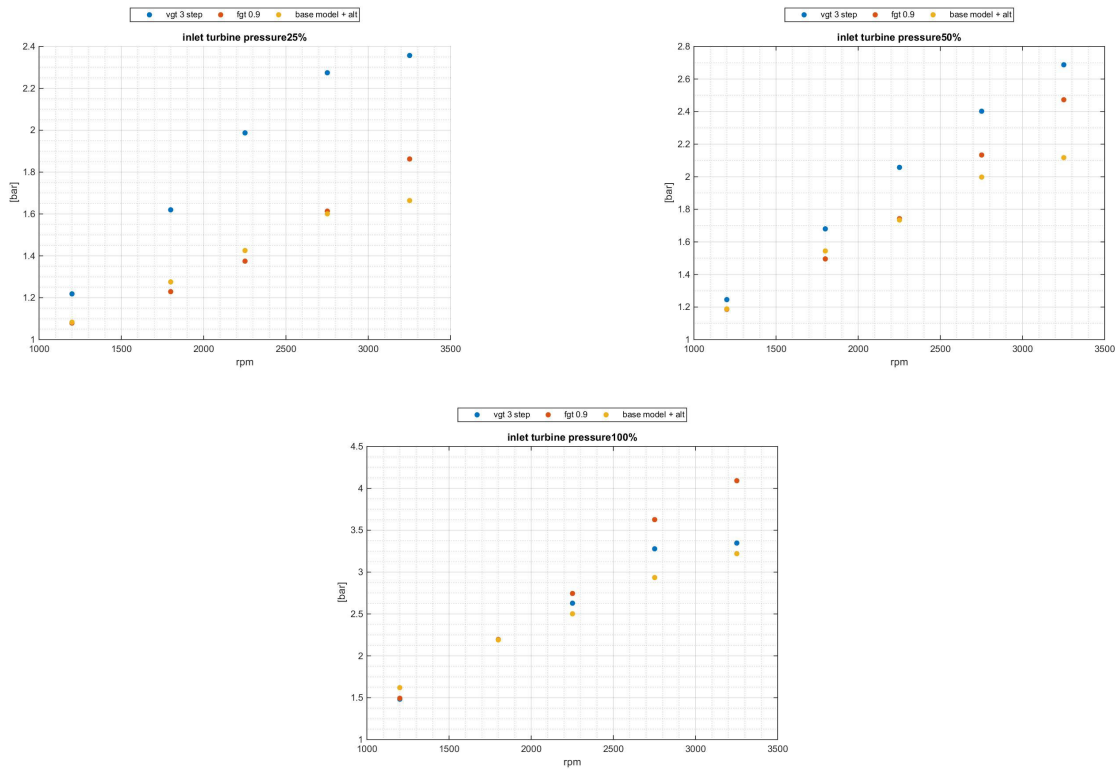


Figure 3.23: Inlet turbine pressure

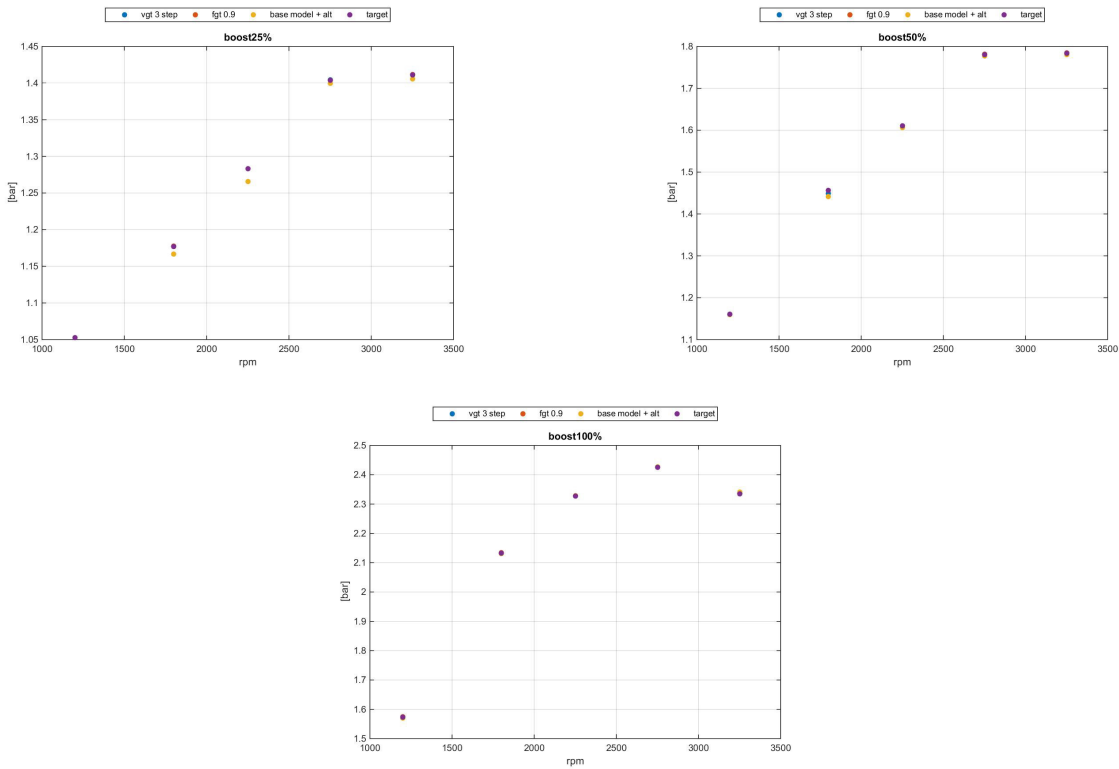


Figure 3.24: Boost pressure

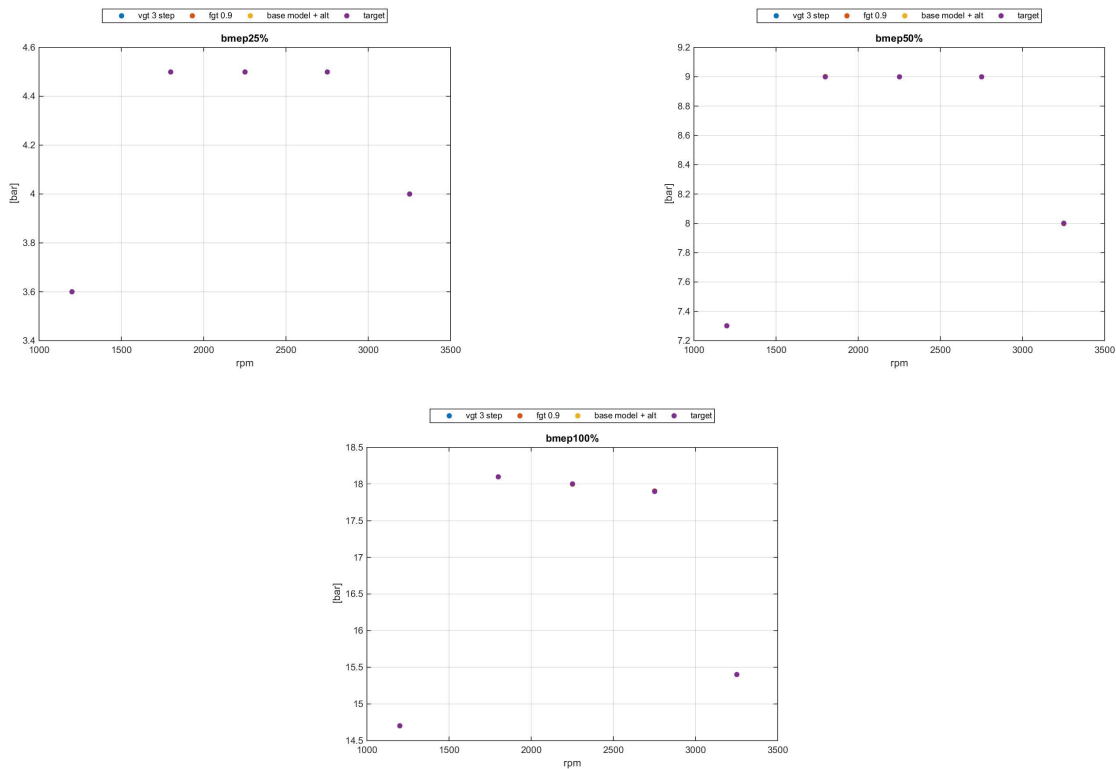


Figure 3.25: Brake mean effective pressure

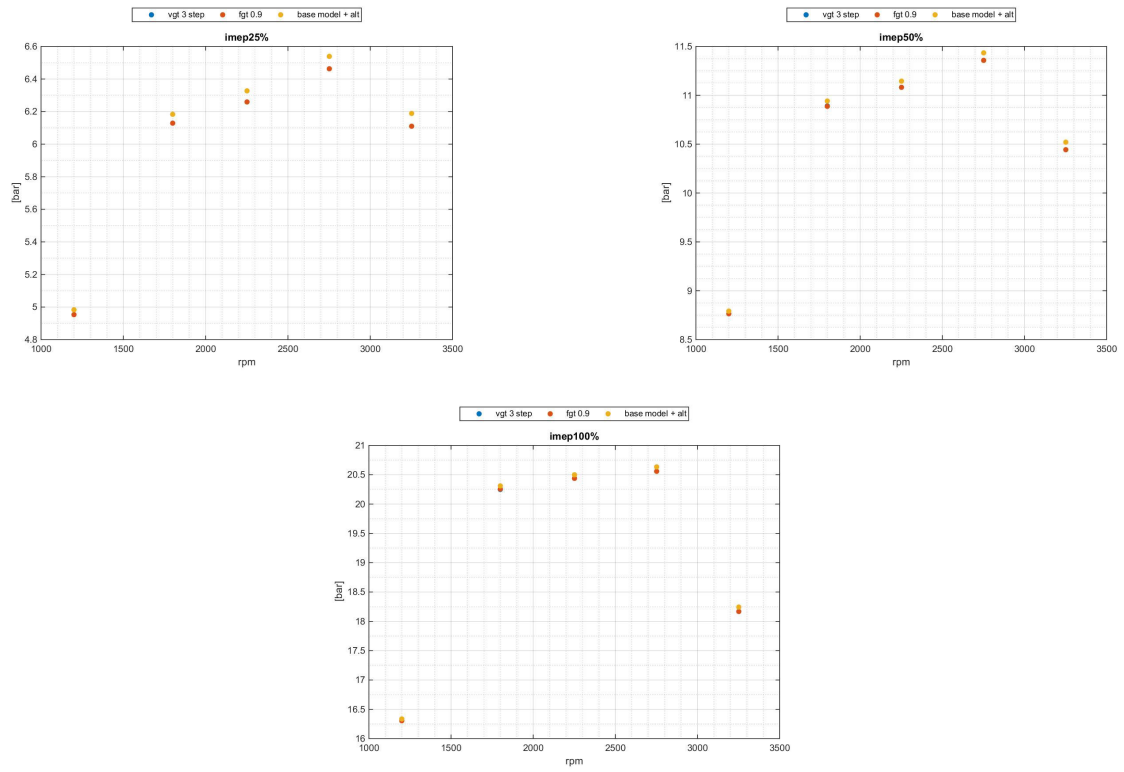


Figure 3.26: Net indicated mean effective pressure

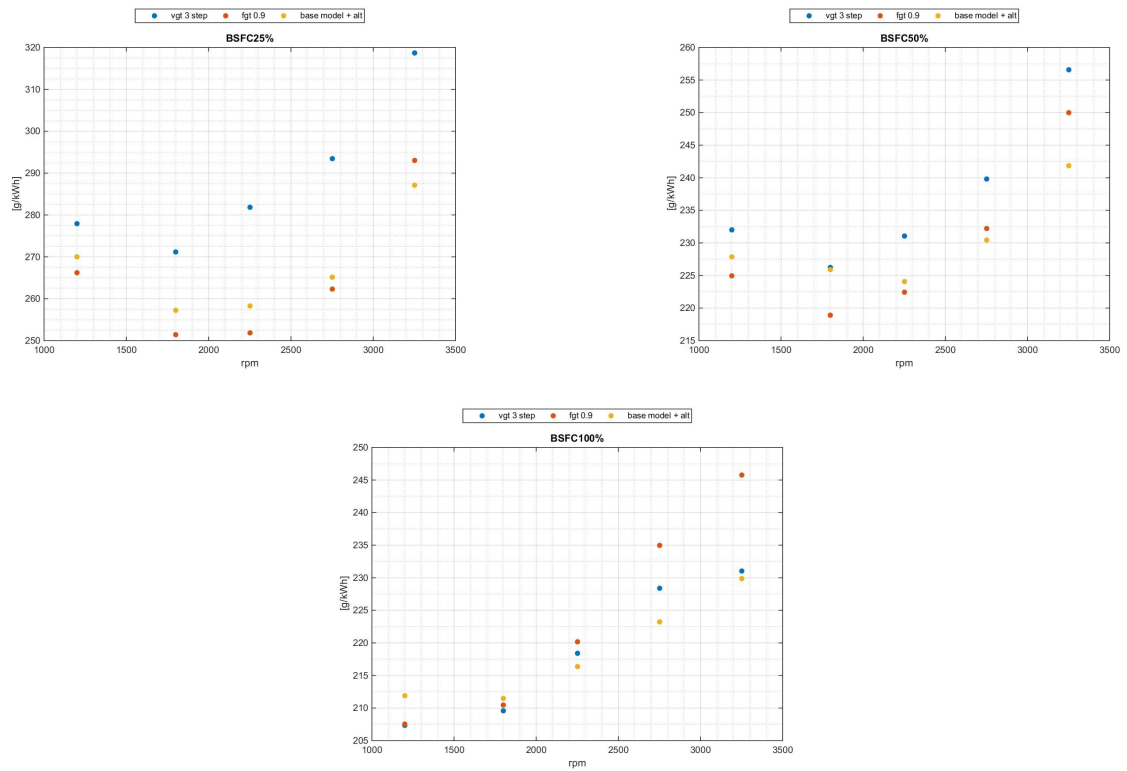


Figure 3.27: Brake specific fuel consumption



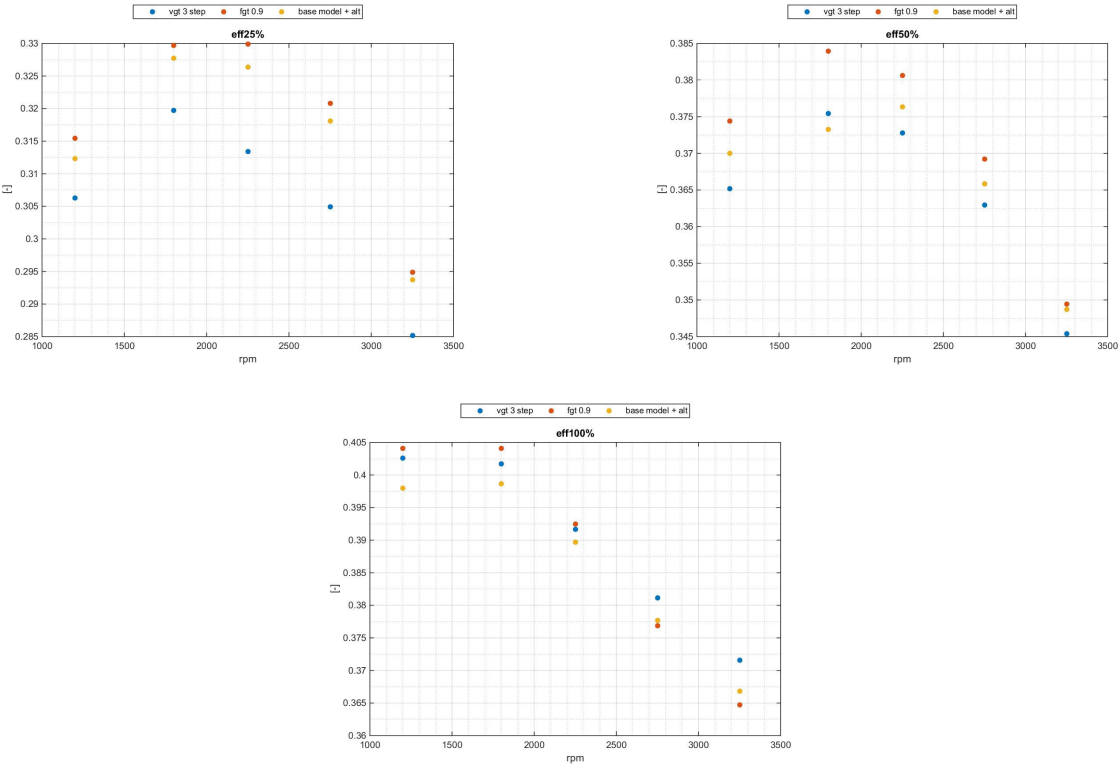


Figure 3.28: System efficiency

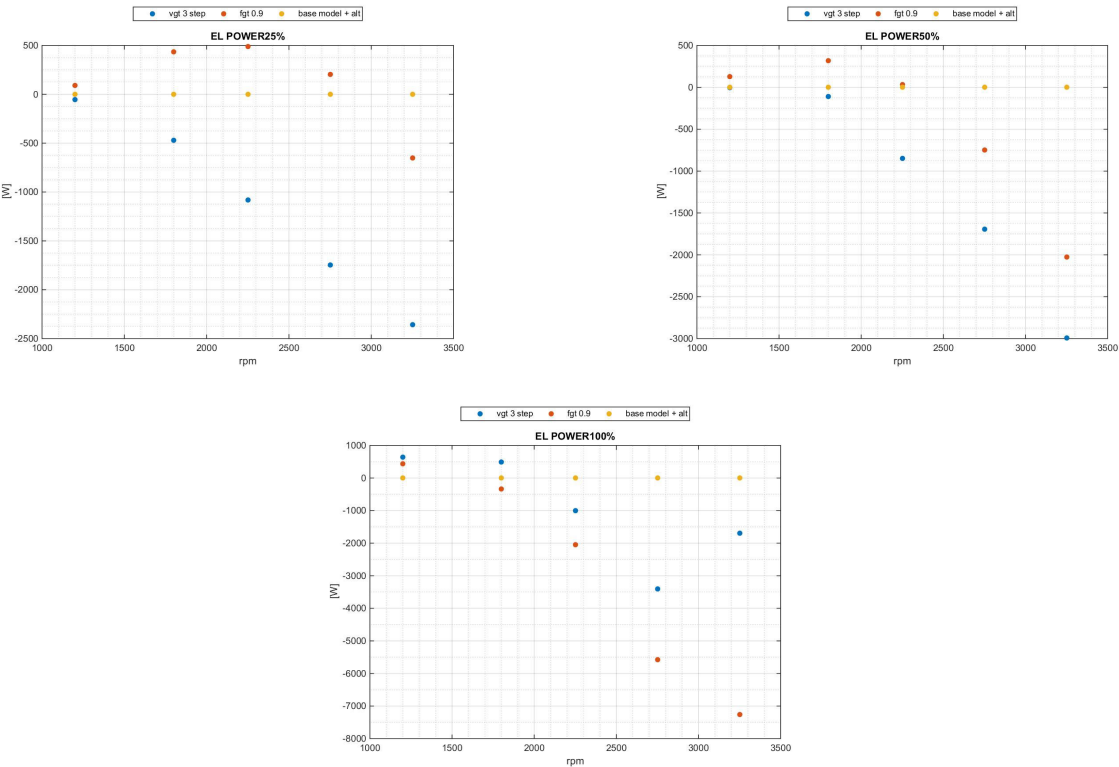


Figure 3.29: Electric power

About back pressure, VGT configuration has always an higher value than "base model", because of the rack position is lower in order to recover more energy in electrical one, with the drawback of higher pmep (pumping mean effective pressure). FGT generates a lower value of back pressure at low engine speeds and greater ones at high engine speeds. With the increase of load, the speed in which the back pressure of FGT configuration becomes higher than "base model" one decreases. Brake specific fuel consumption of VGT is always higher than "base model", due to the higher pmep. This phenomenon is caused by VGT rack position. Indeed, most VGT nozzle is closed, higher is pressure at exhaust port. FGT BSFC has the same trend of back pressure respect the "base model". Efficiency of VGT configuration is worse in partial loads (25% and 50%). In former case the values are about 1% lower, while in latter one the average difference is 0.3%. At full load the efficiency is greater respect the "base model", but with a very small advantage (0.3%). For the FGT configuration is possible to note that the efficiency in every condition is very similar to the reference model, indeed the greater difference is 0.5%. Considering the electrical energy required/recovered, the VGT rack position was fixed in order to recover in every working point, while in FGT configuration at partial loads some electrical power must be required to the battery (25% load between 1200 ÷ 2750 rpm, 50% load between 1200 ÷ 2250 rpm).

### 3.4 DoE

Last step of this work has been to evaluate through the DoE (Design of Experiments) method the real possibility to increase the system efficiency changing some calibration factors. For the two configurations were applied two different DoE types:

- In FGT configuration "Full Factorial Plan" method,
- In VGT configuration "Latin Hypercube" method.

Four working point were analysed, two at 25% and 50% of load respectively. The best and worst efficient points were tested, so to understand how much influence the factors in best and worst conditions. The working points are listed in Tables 3.5 and 3.6:

FGT factors for DoE are: SOI main and Boost pressure. For each factor the level was four, so

FGT	25%	50%
max eff.	2250 rpm	2250 rpm
min eff.	3250 rpm	3250 rpm

Table 3.5: DoE working points FGT

VGT	25%	50%
max eff.	1800 rpm	1800 rpm
min eff.	3250 rpm	3250 rpm

Table 3.6: DoE working points VGT

performing a "Full Factorial Plan" the number of cases to be simulated were sixteen.

The results about this simulations are represented in figures 3.30-3.33 :

In graphs representing the DoE of FGT configuration, green points are the values obtained with the current calibration. Considering the efficiency of engine only (seeing BSFC), it is possible to note that increasing the boost and SOI main (in absolute way), it increases in all points tested. The most influential factor is the boost. SOI main becomes more influential increasing the engine

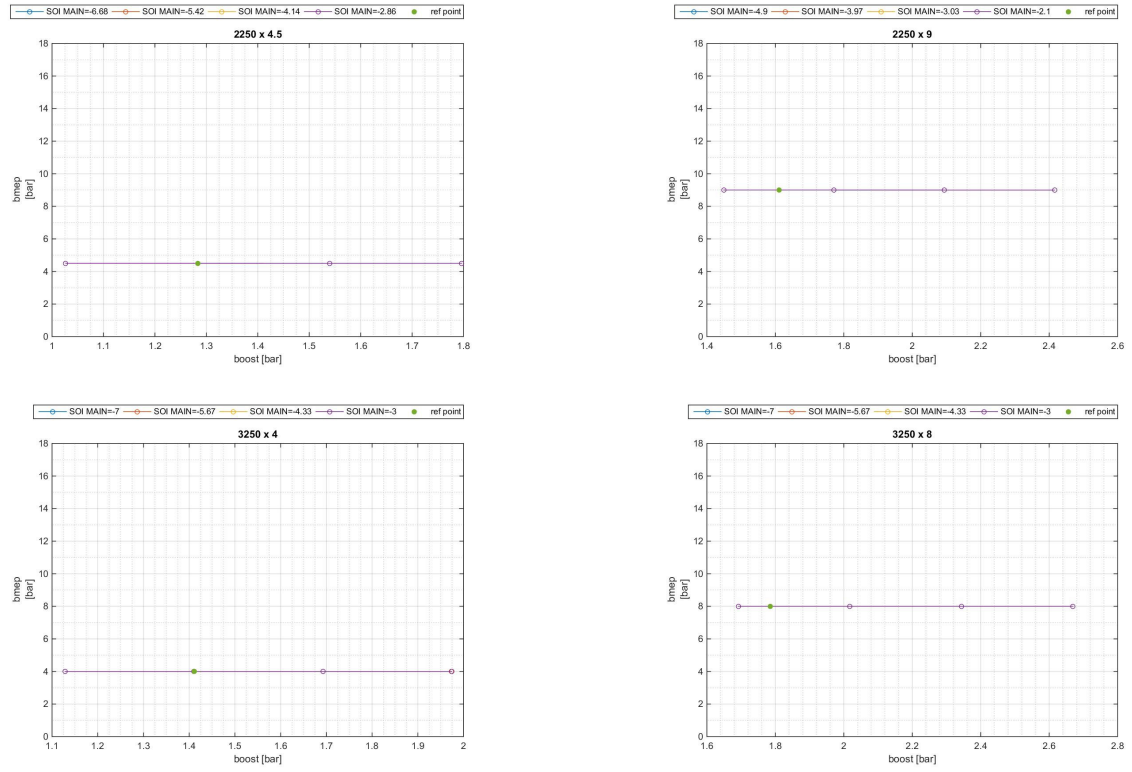


Figure 3.30: Brake mean effective pressure

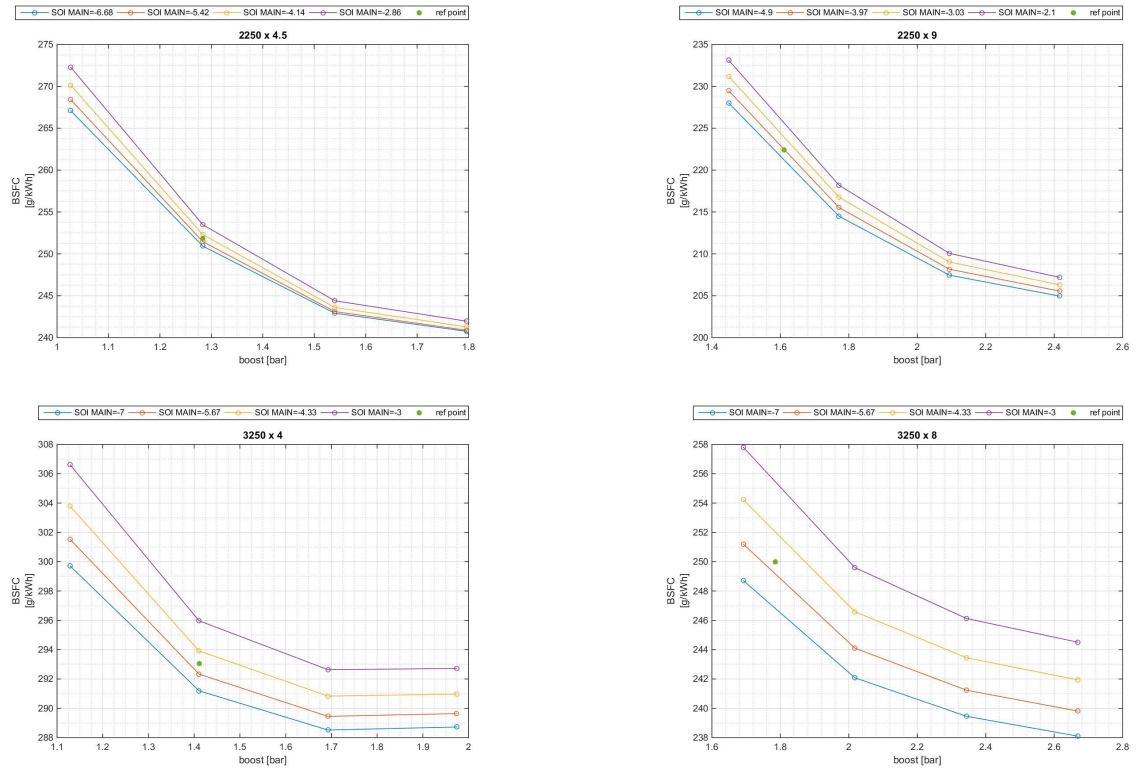


Figure 3.31: Brake specific fuel consumption

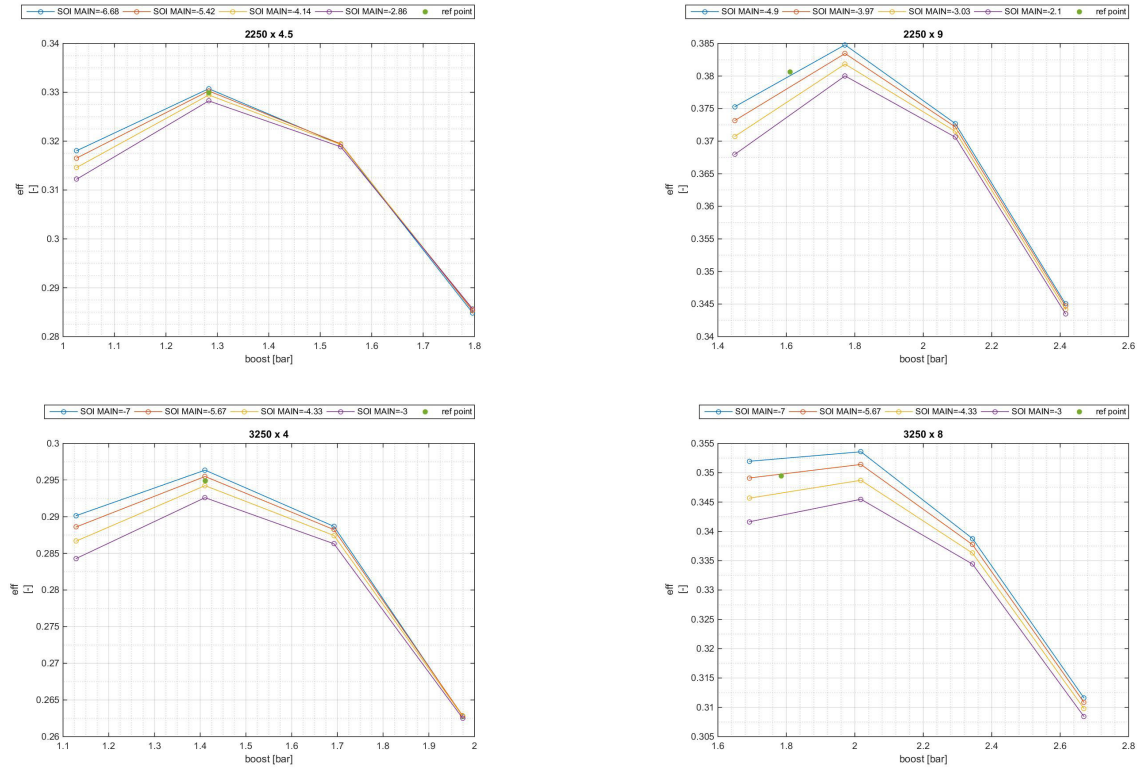


Figure 3.32: System efficiency

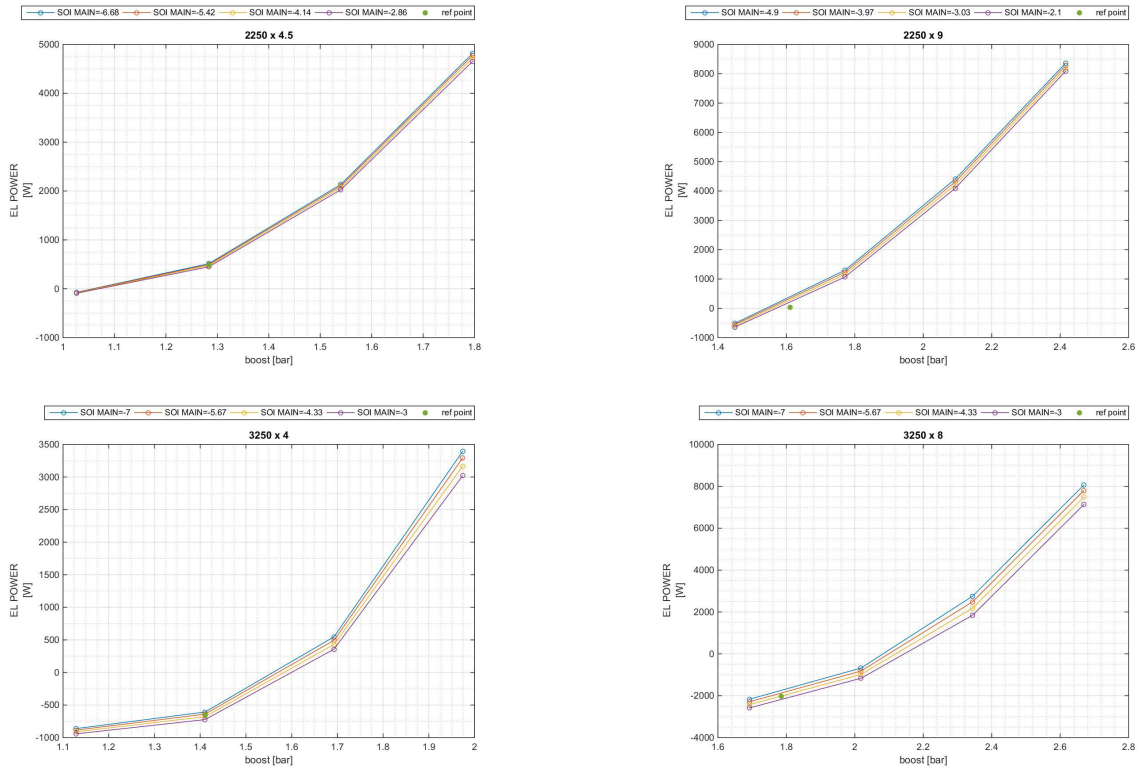


Figure 3.33: Electric power to the battery

speed and the load. To obtain lower BSFC boost must be incremented, but this means that the EM works as motor (Figures 3.33) because exhaust gases energy is not enough to reach too high boost. Indeed, in figures 3.32 one can note that there is a maximum in all plots and then an dramatic decrease of efficiency, in correspondence of an higher electrical power required. Finally observing "ref point" is clear that the factors have been calibrated in optimal way, because they coincide with the maximum or they are very close to them.

VGT factors are three: SOI main, boost and rack position. Performing the "Latin Hypercube plan" 35 cases per each point has been executed. The data are represented below:

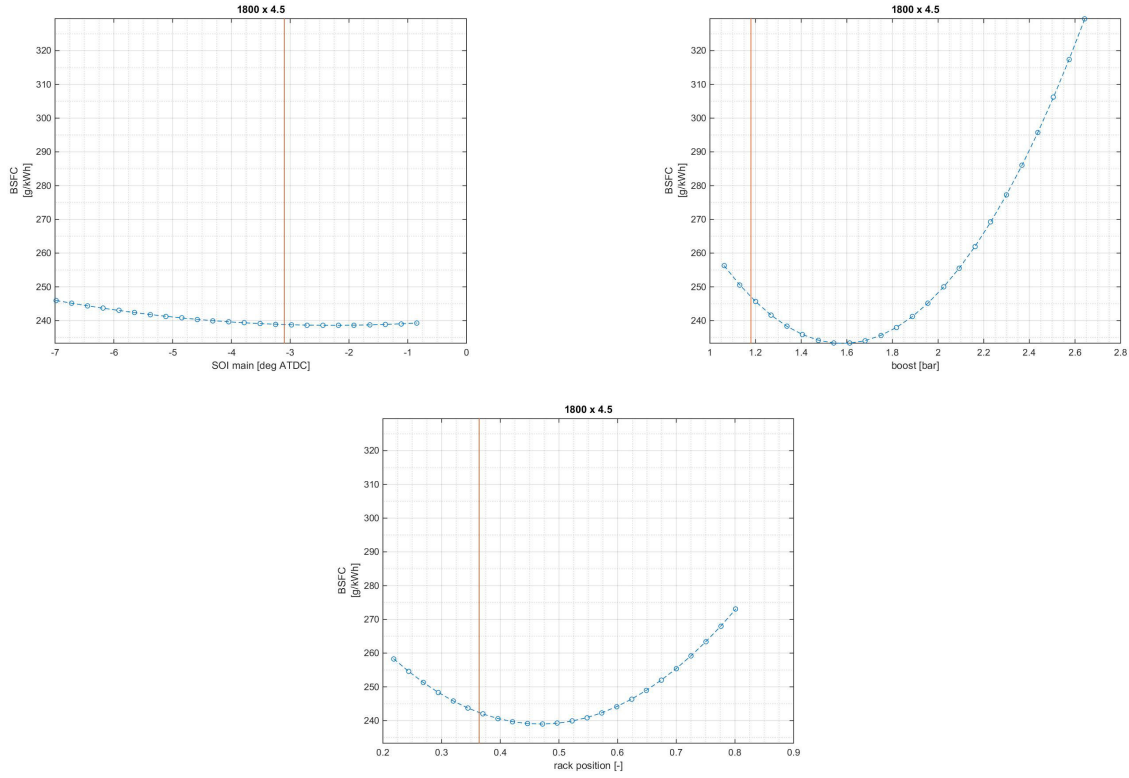


Figure 3.34: Brake specific fuel consumption 1800 x 4.5

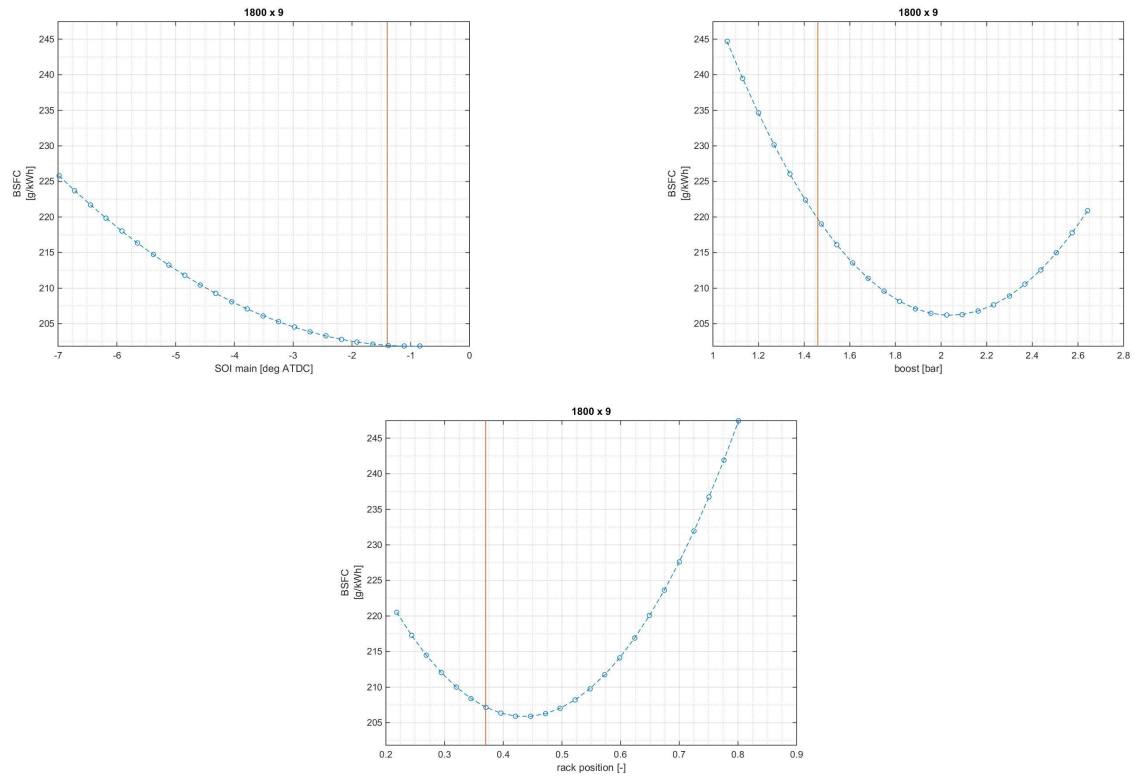


Figure 3.35: Brake specific fuel consumption 1800 x 9

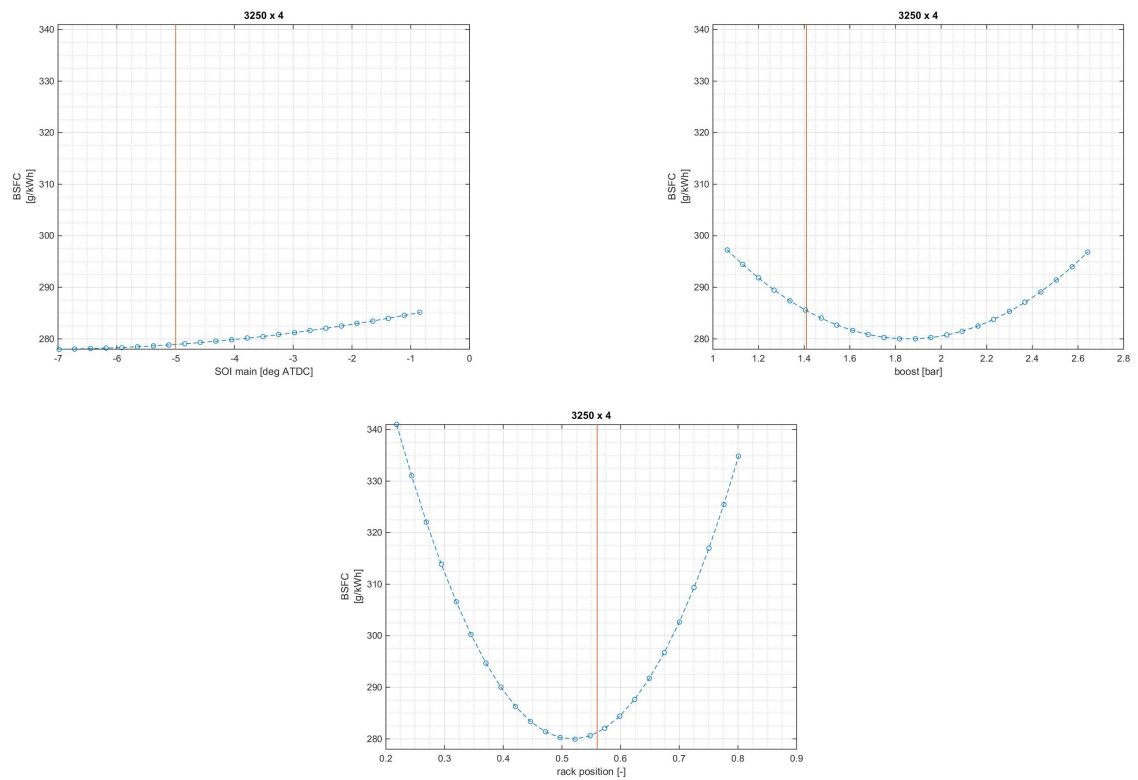


Figure 3.36: Brake specific fuel consumption 3250 x 4



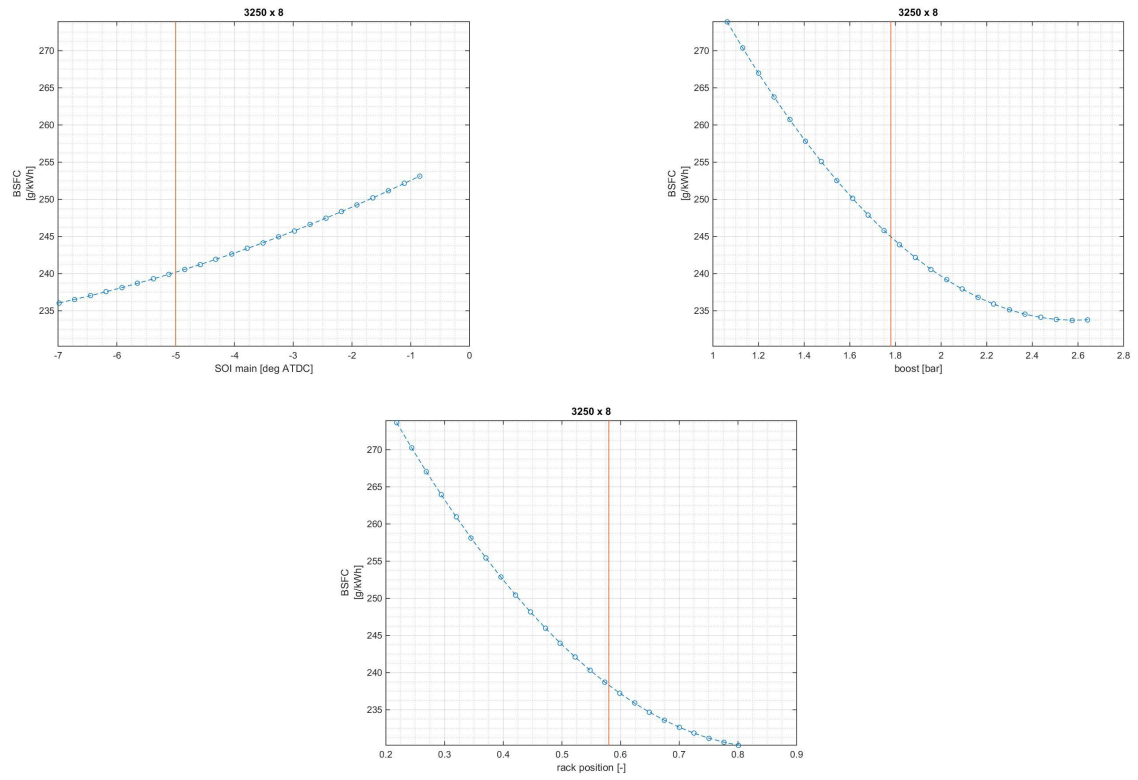


Figure 3.37: Brake specific fuel consumption 3250 x 8

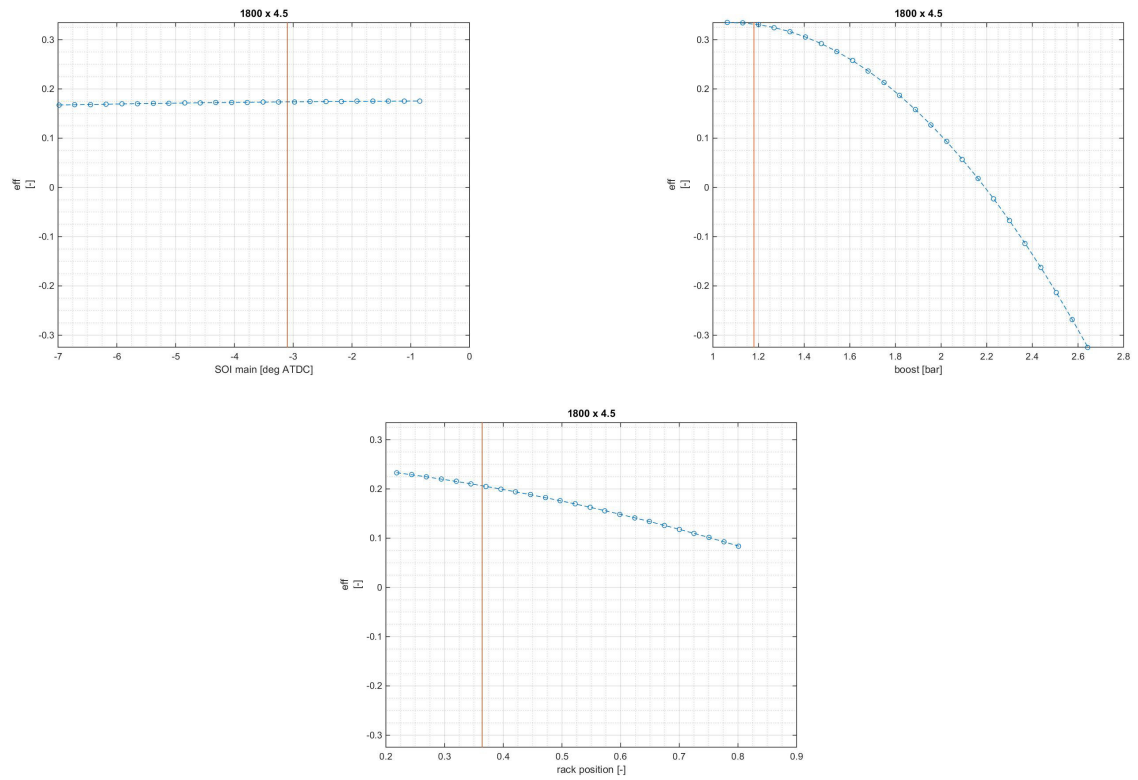


Figure 3.38: System efficiency 1800 x 4.5

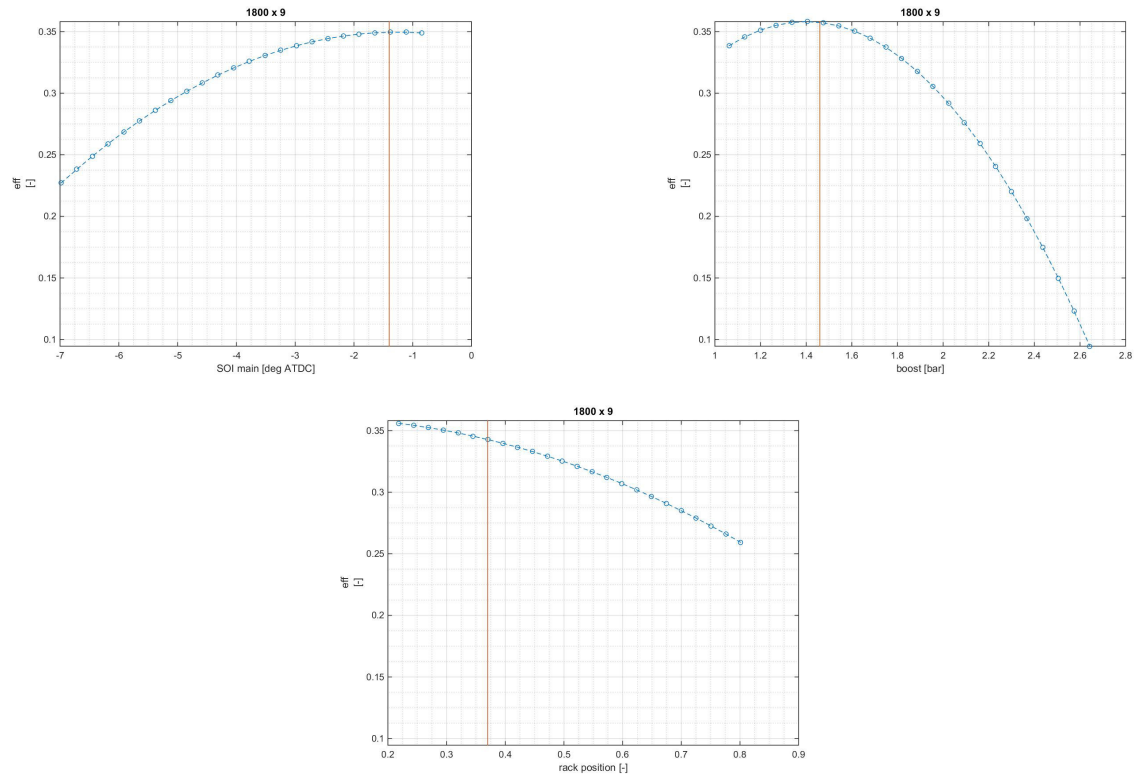


Figure 3.39: System efficiency 1800 x 9

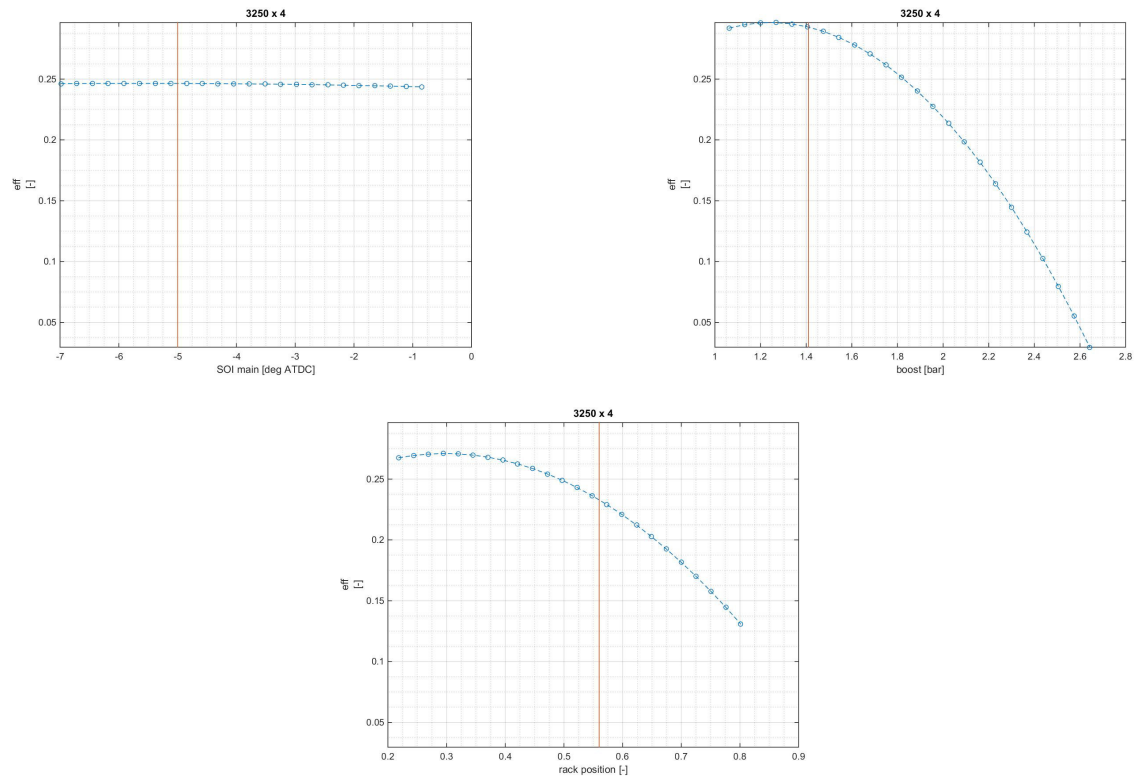


Figure 3.40: System efficiency 3250 x 4



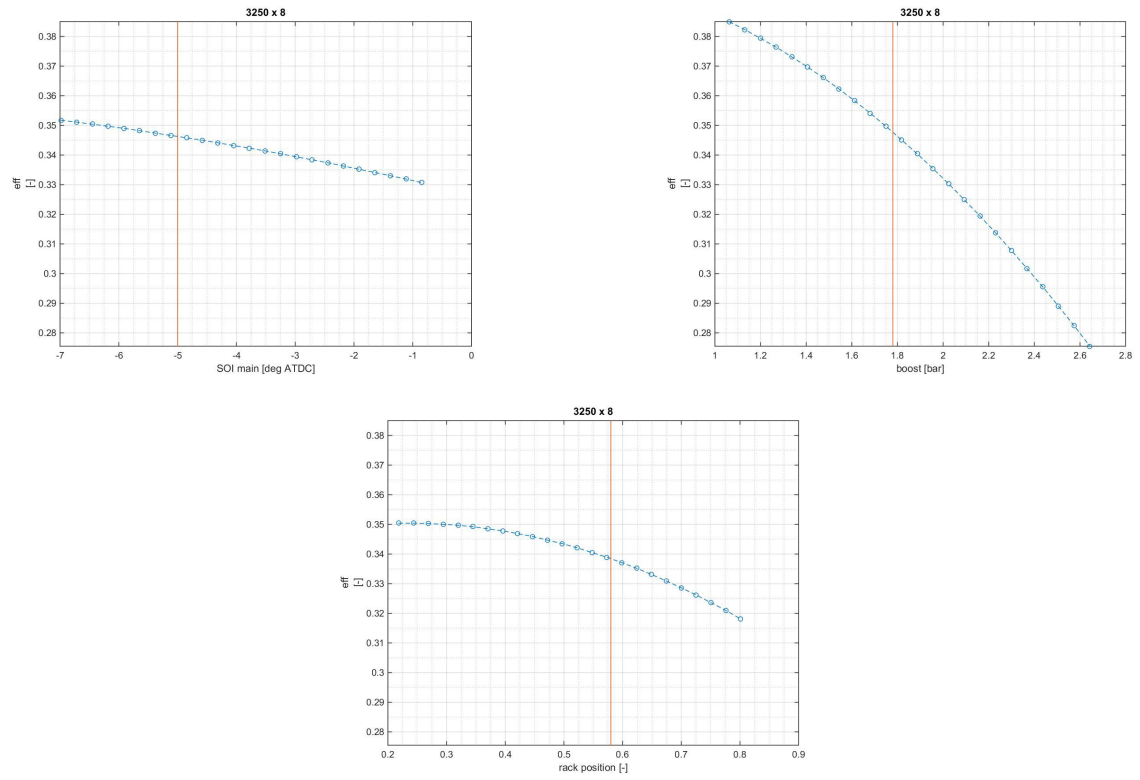


Figure 3.41: System efficiency 3250 x 8

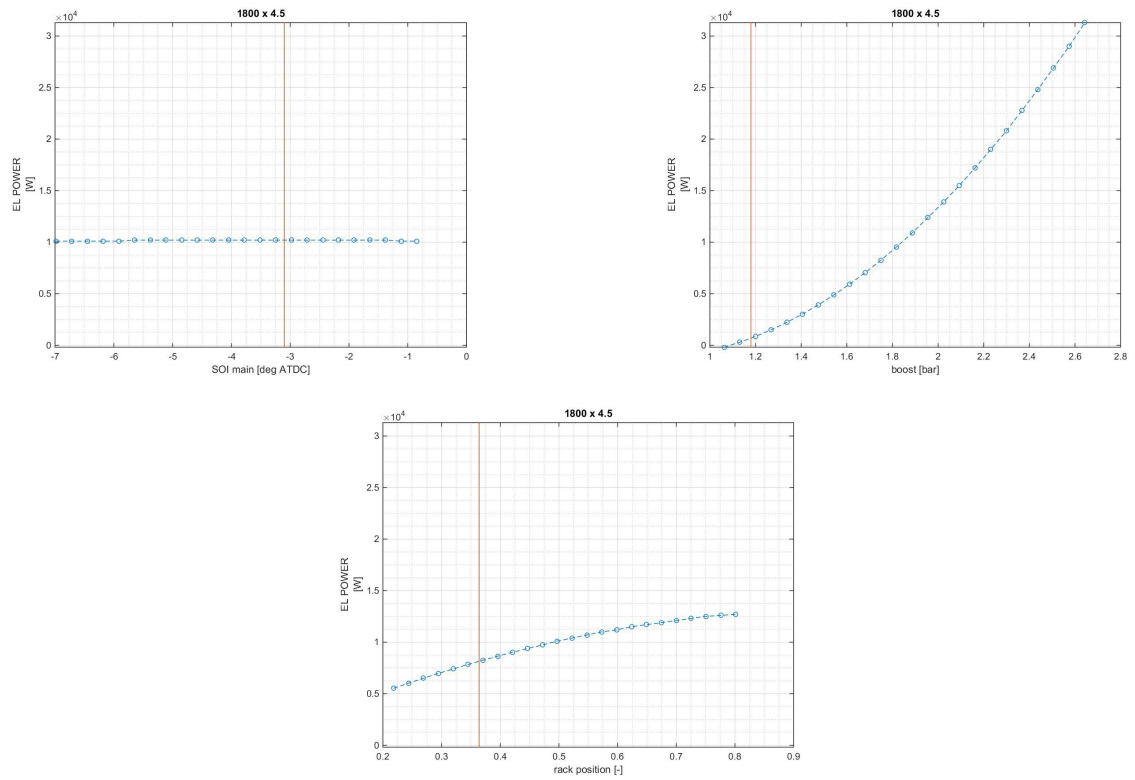


Figure 3.42: Electric power 1800 x 4.5

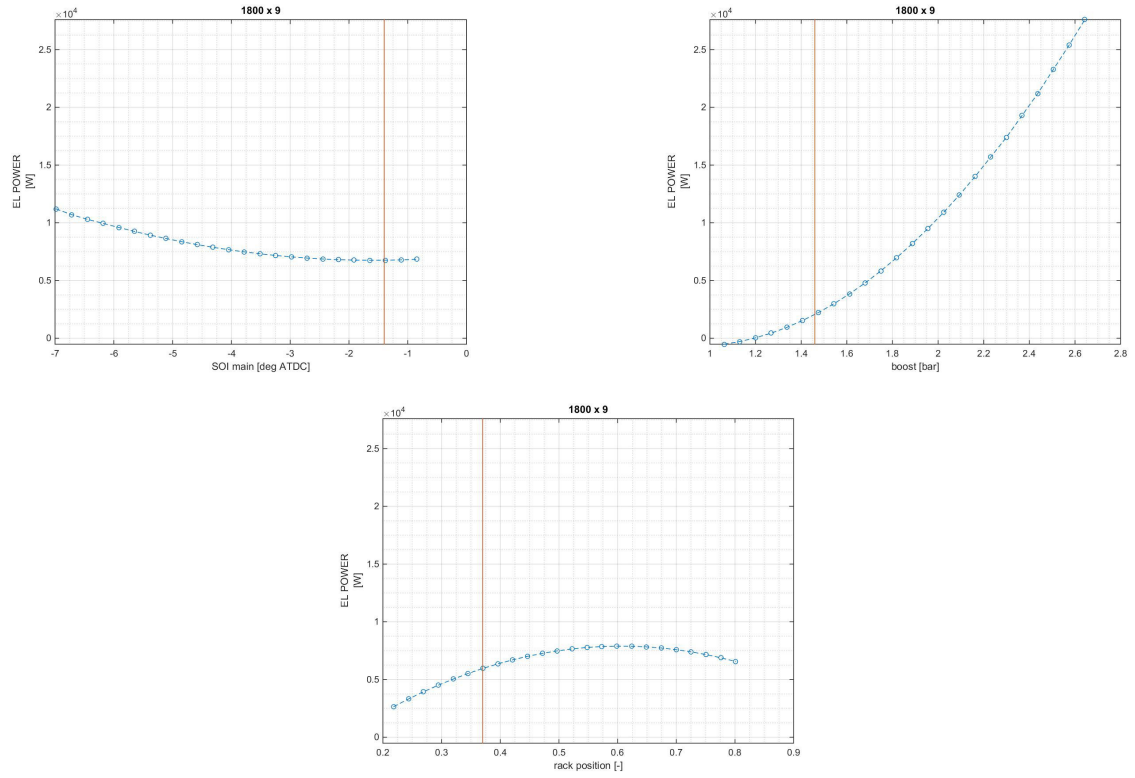


Figure 3.43: Electric power 1800 x 9

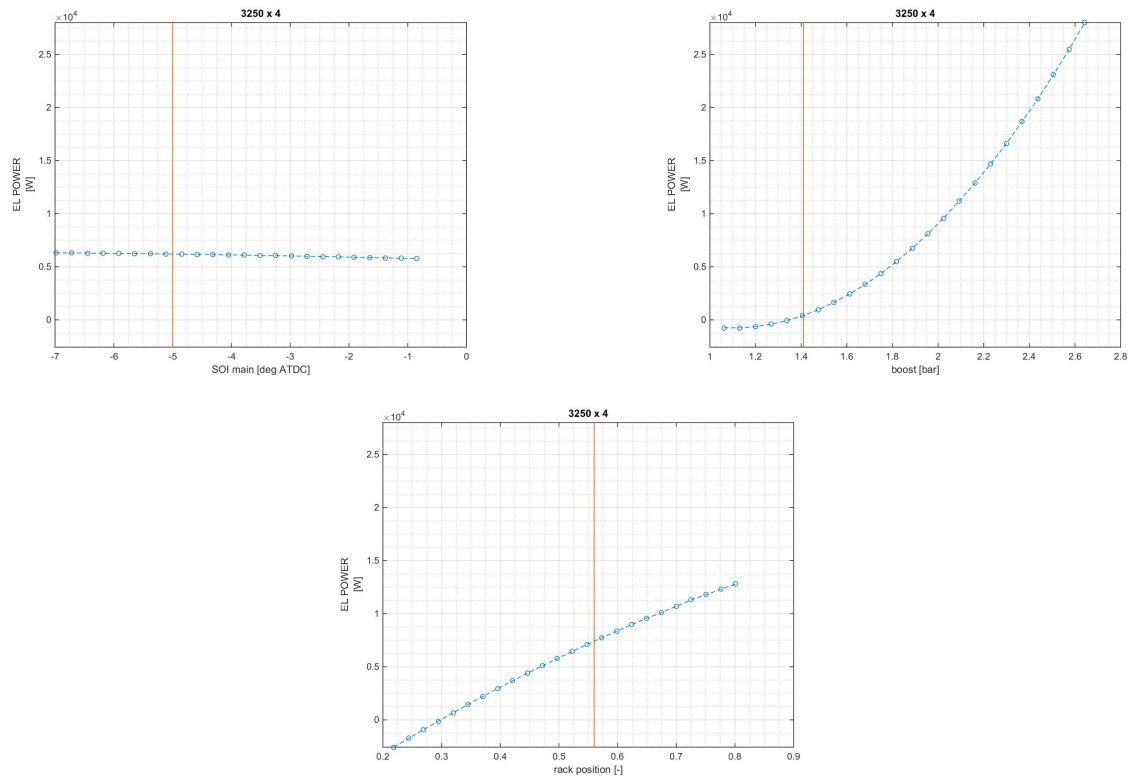


Figure 3.44: Electric power 3250 x 4

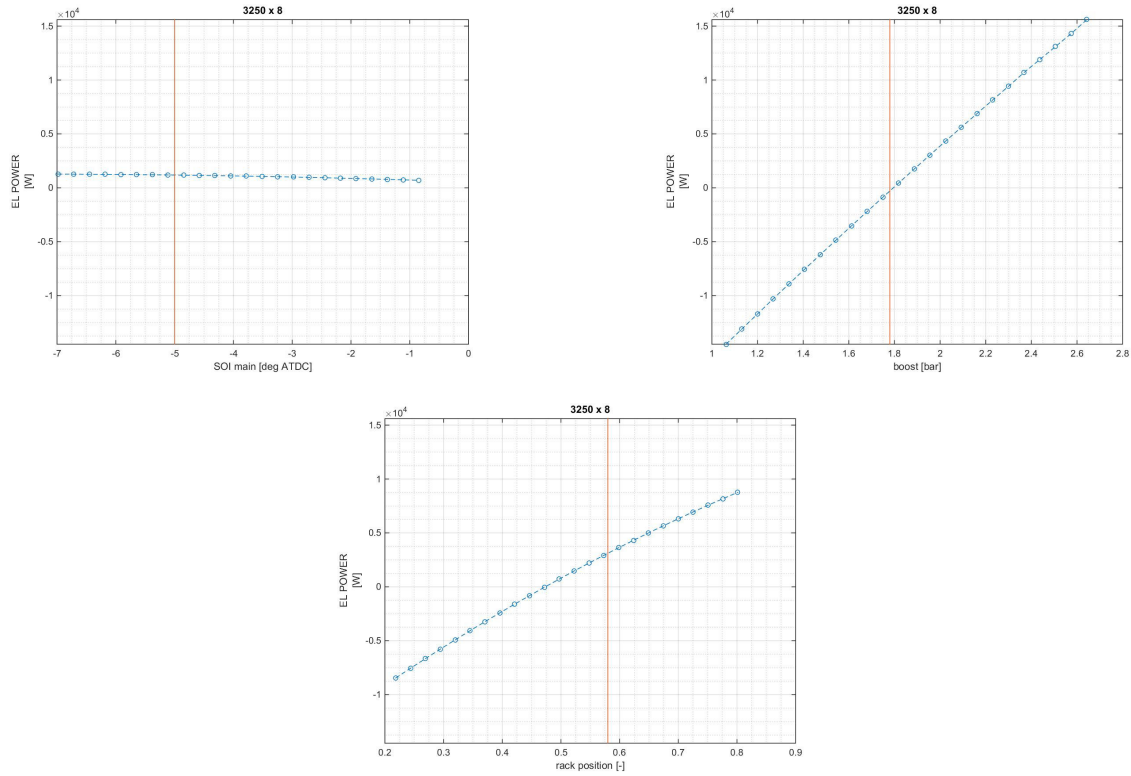


Figure 3.45: Electric power 3250 x 8

The charts represent dependence of parameters (ordinate axis) on the three different factors separately. The red lines represent the factors values at the begin. Analysing BSFC, it is clear that the SOI main is the parameter less influential. BSFC becomes more dependent on SOI main with the increase of load. The other 2 factors have parabola trend, and the minimum is close to the starting calibration point, this means that about the engine efficiency, factors have been calibrated to obtain a low fuel consumption. Concerning the efficiency of whole system, the SOI main at 25% of load has no influence, while it becomes relevant at 50%. Boost and rack position has a greater influence, boost is the major one. Also in these plots it is evident that the calibration is very close to maximum efficiency; indeed only in working point 3250 rpm and 8 bar there is a margin in which it could increase in sensitive way.

# Chapter 4

## Conclusion

### 4.1 Final Remarks and future works

The aim of this thesis was to evaluate the performance of a diesel engine used for commercial vehicle equipped with an electrified turbocharging system (e-turbo). The investigation was carried out using the GT-power commercial software. In particular, the e-turbo system is able to recover part of the energy of the exhaust gases, which can be stored in a battery and used, for example, to drive electrified accessories (e.g., fuel pump, oil pump, water pump were electrified in this study). The potential of the e-turbo system in increasing the powertrain efficiency was analyzed, also by exploring different types of turbine configuration (VGT, i.e., variable geometry turbine and FGT, i.e., fixed geometry turbine) or different sets of engine calibration parameters. Moreover, with reference to the FGT case, different turbine sizes were explored by using a scaling factor to modify the characteristic map (these cases are denoted with FGT 0.8, FGT 0.9, FGT 1 and FGT 1.1). The results show that the energy recovered thanks to the electric turbo with FGT is not enough to power the oil pump, the water pump and the fuel pump. Indeed, only the smaller configuration (FGT 0.8) satisfies the power demand, at full load conditions, from 2250 rpm and with lower powertrain efficiency than the "base model". Also the possibility to replace the alternator with the e-turbo system was explored, but it was found that this is not possible because the energy which is recovered by the e-turbo system is higher than that generated by the alternator only at full load conditions and from a speed of 1800 rpm. A solution available is to use the oil pump and the water pump with the VGT turbine, where in almost all points simulated the power needed is recovered by the electric turbo. It was also verified that To obtain sufficient electrical power to drive the oil and water pump with the FGT turbine configuration a change in boost target is required.

As previously stated, also the effect of the main engine calibration parameters on the powertrain efficiency was explored, by means of a DoE (Design of Experiment) technique. However, it was found that the baseline engine calibration dataset is very close to the optimal one.

Finally, one can conclude that gain in powertrain efficiency which can be achieved using an e-turbo system on the considered engine is very small. Instead, a great advantage of an e-turbo system consists in the possibility of reducing the turbo-lag in transient operation (this aspect, however, was not investigated in the present thesis).

An other development could be reached using electric water pump. Indeed thanks the decoupling between engine speed and the pump speed it is possible to manage the coolant system in an optimal way in every condition (e.g. to reduce the warm up time remaining water pump off so that the coolant reach target temperature in lower time).

The electrification of internal combustion engine is one of the main fields of interest for all automotive OEMs. In case of the engine simulated and analysed in this thesis could be tested the possibility to mount an electric turbo compound like in figure 1.3, or analyse an engine of greater dimensions.

# Chapter 5

## Further plots

In this last chapter some additional plots are shown.

### 5.1 Turbomatching plots

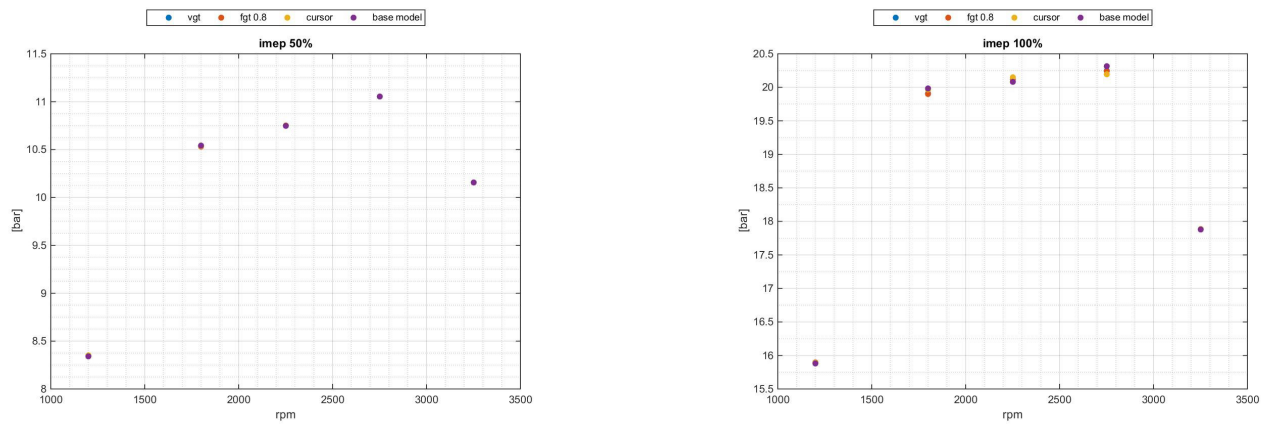


Figure 5.1: Indicative mean effective pressure

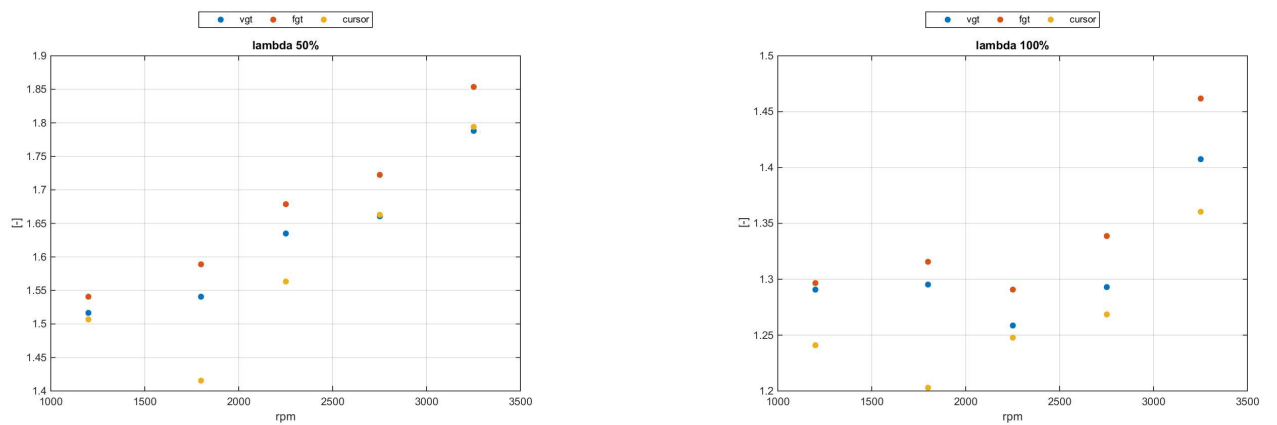


Figure 5.2: Lambda coefficient

## 5.2 FGT and EM

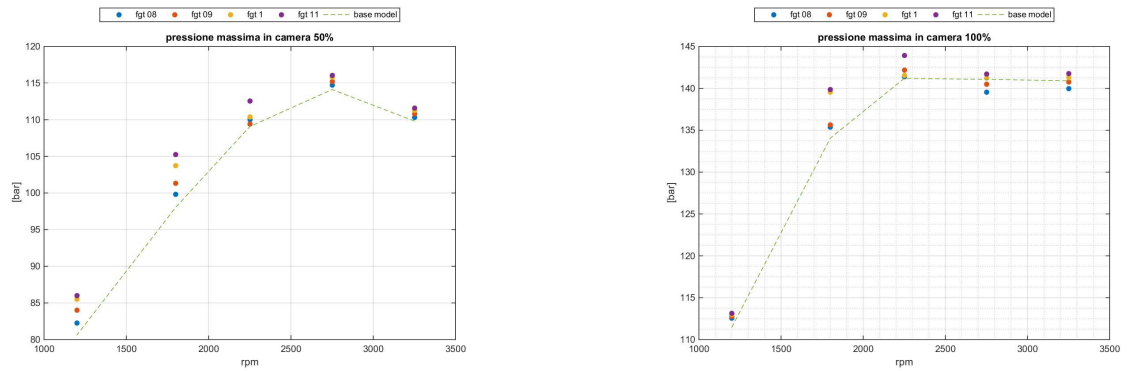


Figure 5.3: Maximum pressure in combustion chamber

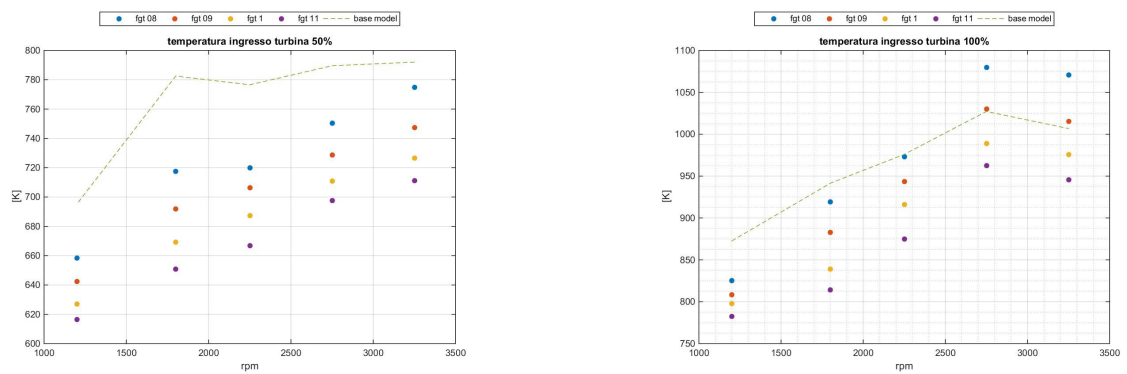


Figure 5.4: Inlet turbine temperature

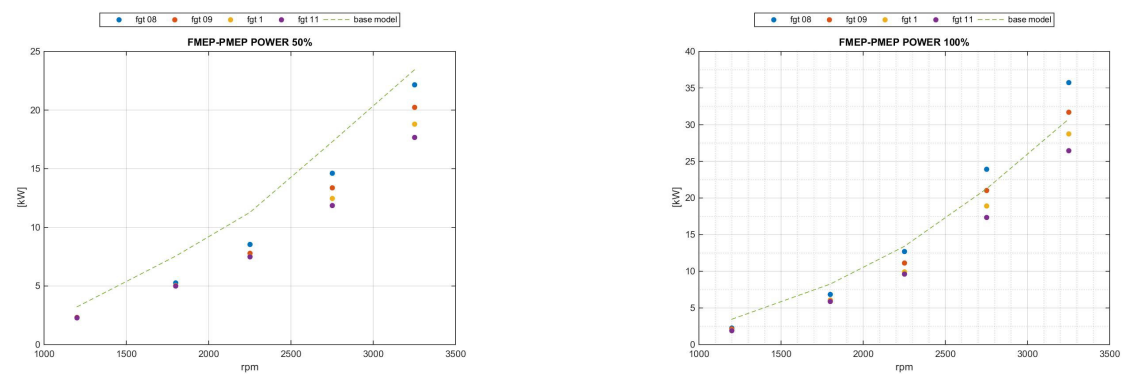


Figure 5.5: Total power dissipated

## 5.3 Accessories division

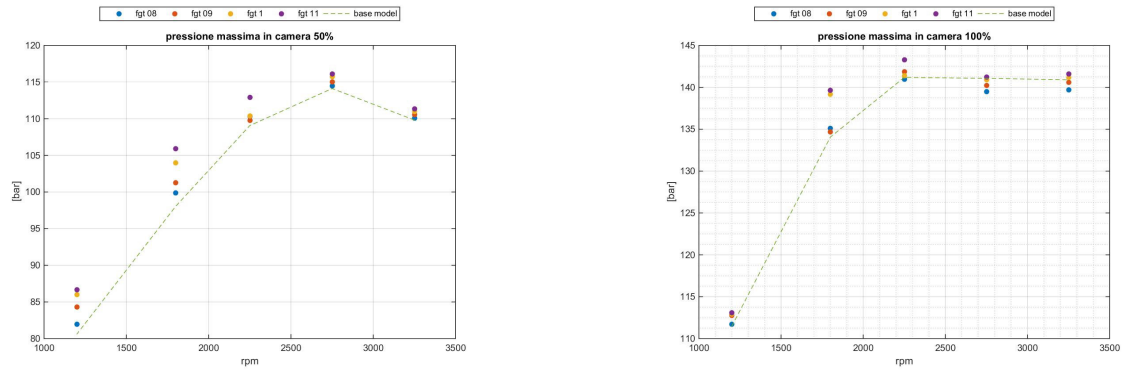


Figure 5.6: Maximum pressure in combustion chamber

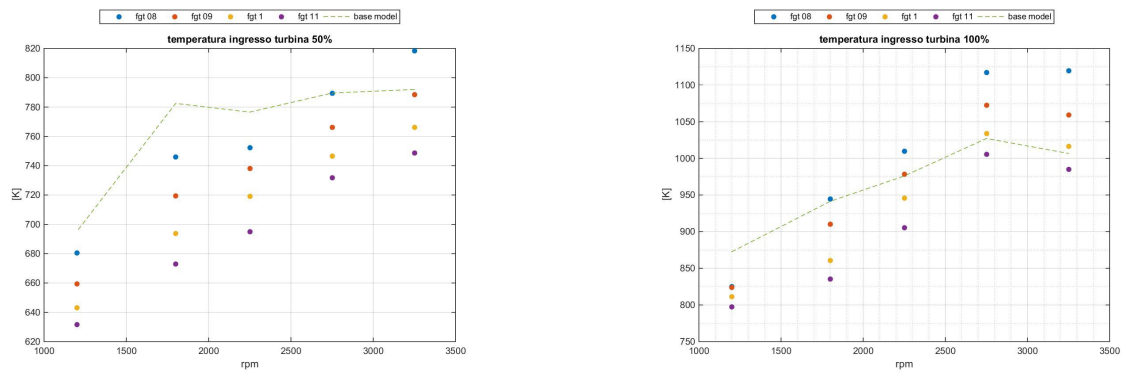


Figure 5.7: Inlet turbine temperature

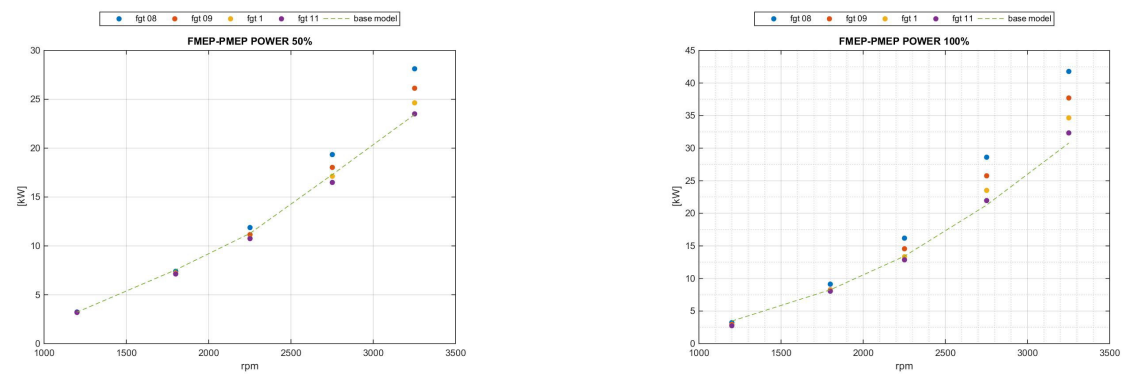


Figure 5.8: Total power dissipated

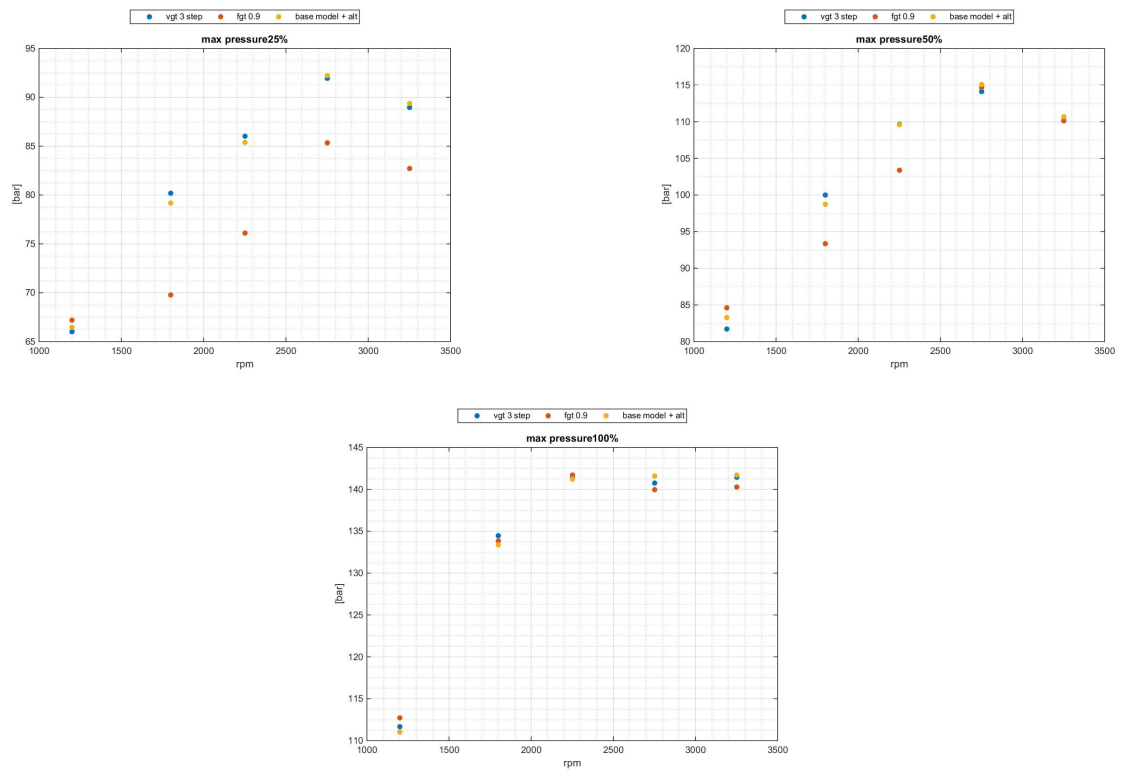


Figure 5.9: Maximum pressure in combustion chamber

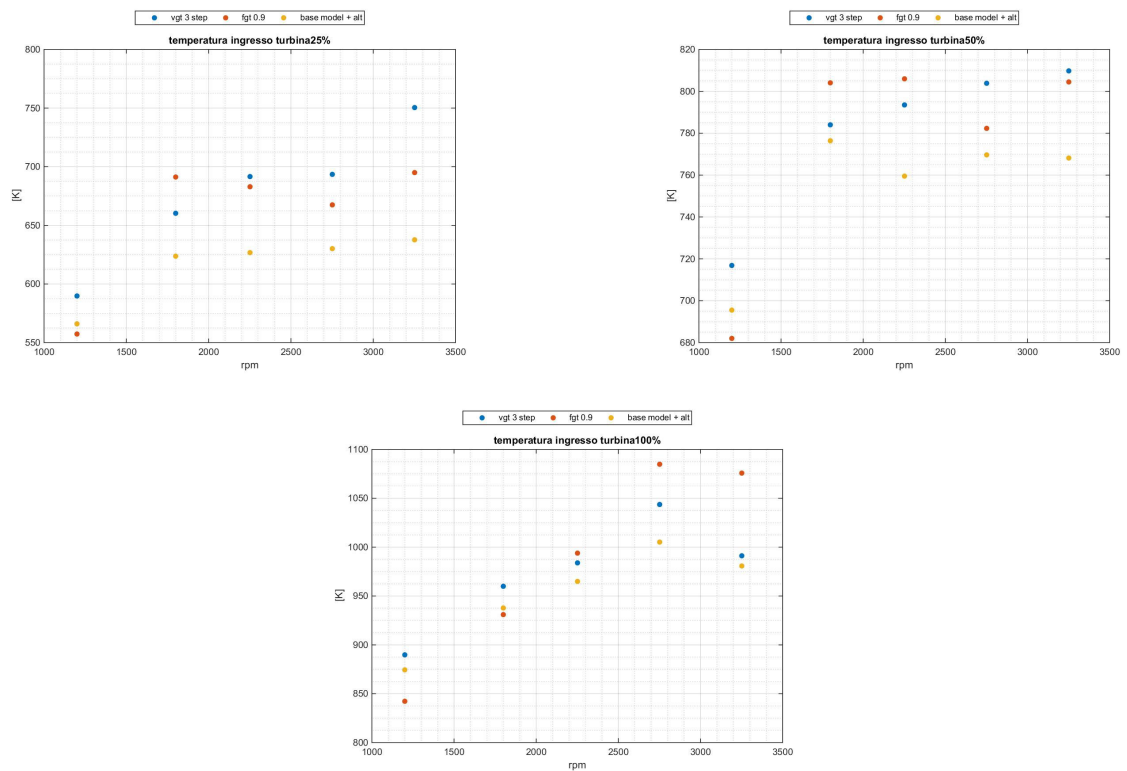


Figure 5.10: Inlet turbine temperature



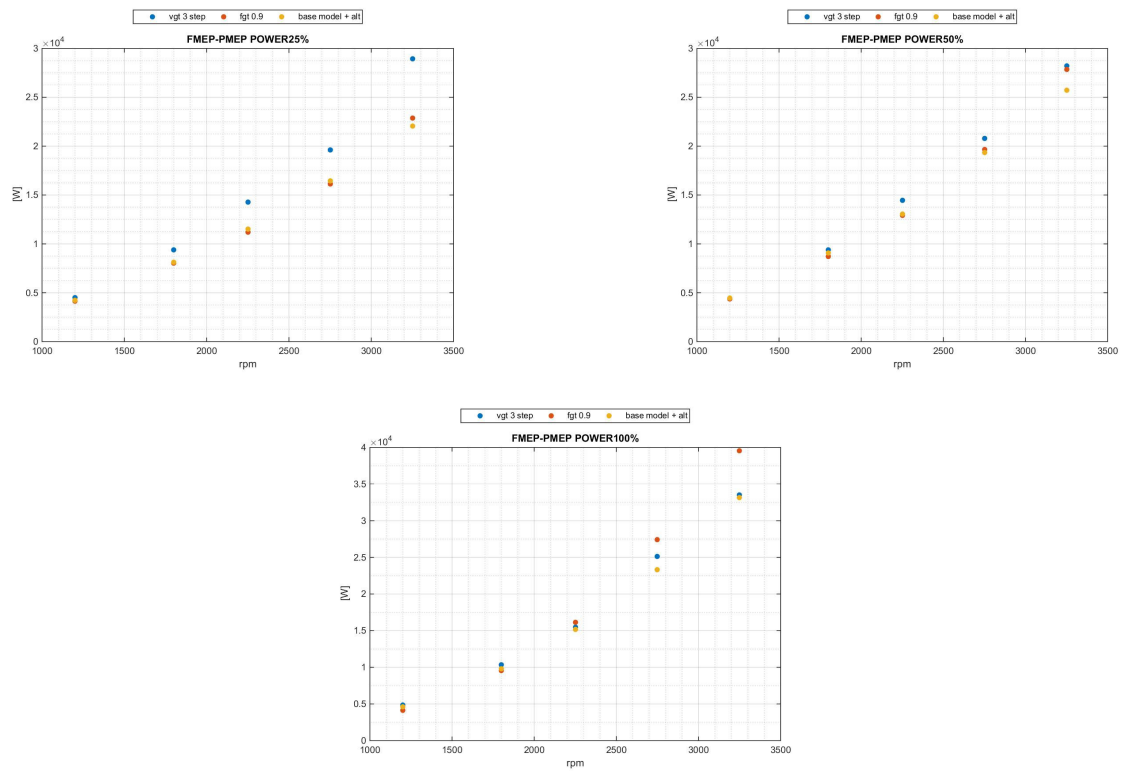


Figure 5.11: Total power losses

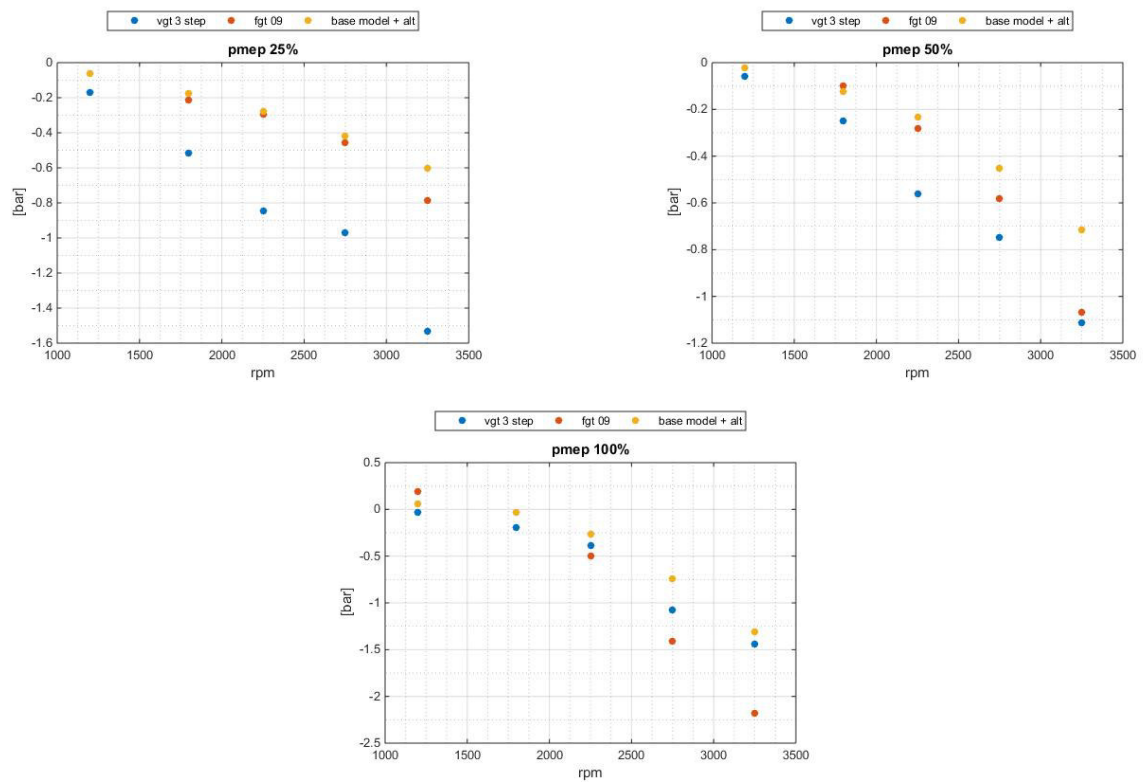


Figure 5.12: Pumping mean effective pressure

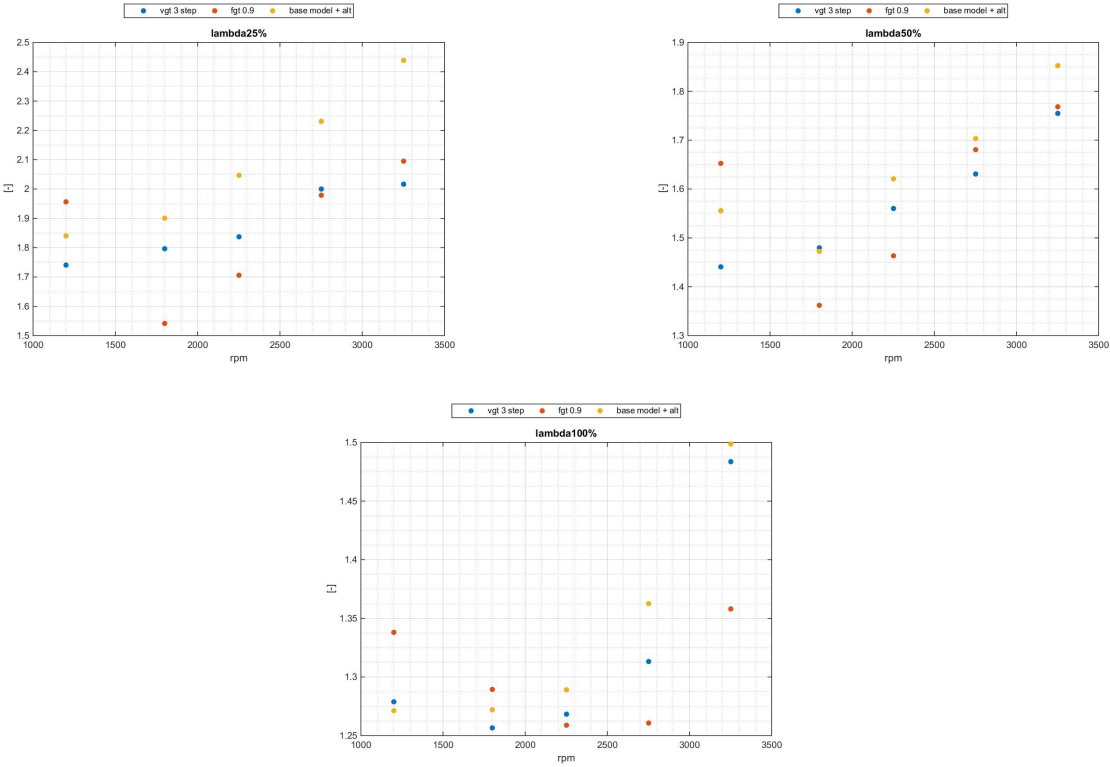


Figure 5.13: Lambda coefficient